Fall 2009

An Analytical Investigation of Natural Frequency for a Symmetric Composite Box-Beam with Thermal Effects

Lakshmi Narayana Sanjeev Chitikela
Embry-Riddle Aeronautical University - Daytona Beach

AN ANALYTICAL INVESTIGATION OF NATURAL FREQUENCY FOR A SYMMETRIC COMPOSITE BOX-BEAM WITH THERMAL EFFECTS

by

Lakshmi Narayana Sanjeev Chitikela

A Thesis Submitted to the Graduate Studies Office
In Partial Fulfillment of the Requirement for the Degree of
Master of Science in Aerospace Engineering

Embry-Riddle Aeronautical University
Daytona Beach, Florida
Fall 2009

AN ANALYTICAL INVESTIGATION OF NATURAL FREQUENCY FOR A SYMMETRIC COMPOSITE BOX-BEAM WITH THERMAL EFFECTS

by

Lakshmi Narayana Sanjeev Chitikela

This thesis was prepared under the direction of the candidate's committee chairman, Dr. Habib Eslami, Department of Aerospace Engineering, and has been approved by the members of his thesis committee. It was submitted to the School of Graduate Studies and was accepted in partial fulfillment of the requirements for the degree of Master of Science in Aerospace Engineering.

THESIS COMMITTEE:

Dr. Habib Eslami
Chairman

Dr. Frank J. Radosta
Member

Dr. Sathya Gangadharan
Member

Dr. Habib Eslami,
Chair, Aerospace Engineering Department

3/29/10
Date

Dr. James Cunningham
Associate Vice President for Academics

3/31/10
Date

ACKNOWLEDGEMENTS

I sincerely express my deep gratitude to my thesis advisor Dr. Habib Eslami, Professor and Chair of Aerospace Engineering Department for his constant guidance, encouragement and support throughout this research. I have learned many things since I became Dr. Eslami's student.

I also thank my thesis committee members Dr. Frank J Radosta and Dr. Sathya Gangadharan for sparing their valuable time and editing.

The most special thanks goes to my parents and friends, for their unconditional support and love through all this long process.

Lakshmi N. Sanjeev Chitikela

15th February, 2010

This work is dedicated to my family and teachers

ABSTRACT

Author: Lakshmi Narayana Sanjeev Chitikela

Title: An Analytical Investigation of Natural Frequency for a Symmetric Composite Box-Beam with Thermal Effects

Institution: Embry-Riddle Aeronautical University

Degree: Master of Science in Aerospace Engineering

Year: 2009

The main purpose of the following analysis is to develop an analytical method for determining the natural frequency of a symmetric composite box-beam subjected to temperature gradient. A set of coupled partial differential equations of motion is obtained by means of small defection theory and D'Alembert's method. The Smith and Chopra stiffness matrix is used in the governing equations of motion and an appropriate MATLAB® code has been written to solve for the stiffness matrix elements of the box-beam. The resulting governing equations of motion are solved to obtain the natural frequencies of the box-beam in flap and lag directions using Galerkin's method. Finally, an example solution for symmetric composite box-beam of [+45°; ±45°] layup using cantilever boundary conditions is presented. For validation of the current analysis, comparisons are made with previously published results.

Table of Contents

List of Figures

List of Tables

Page

Nomenclature

c x d	Inner cross-sectional dimensions
l	length of the beam
m	mass of blade per unit length
$p_{(\,)}$	Inertial forces
$q_{(\,)}$	Inertial Moments
t	time
u	Axial deformation due to extension
v	Horizontal deformation due to bending
w	Vertical deformation due to bending
A	Cross-sectional area of a box-beam
A_{ij}	Laminate in-plane stiffness matrix
K	Stiffness matrix of box-beam
K_A	Effective polar radius of gyration of blade cross-section $(\sqrt{(I_{yy}+I_{zz})/A})$
$K_{m1\ m2}$	Principle mass radii of gyration of blade cross-section
K_{11}	Axial stiffness
K_{12}	Extension-chordwise shear coupling stiffness
K_{13}	Extension-spanwise shear coupling stiffness
K_{14}	Extension-torsion coupling stiffness
K_{22}	Chordwise shear stiffness coupling
K_{33}	Spanwise shear stiffness coupling
K_{44}	Torsional stiffness
K_{45}	Bending-torsion (spanwise) stiffness coupling

K_{46}	Bending-torsion (chordwise) stiffness coupling
K_{55}	Spanwise bending stiffness coupling
K_{66}	Chordwise bending stiffness coupling
$M_{()}$	Moments acting on the box-beam
Q	Ply stiffness matrix
ΔT	Change in temperature (Temperature difference)
U	Total axial deformation
V	Total horizontal deformation
V_x	Axial force acting on the box-beam
$V_{()}$	Shear force acting on the box-beam
W	Total vertical deformation
α	Non-dimensional warping factor
$\alpha_{()}$	Co-efficient of thermal expansion
β	Non-dimensional warping parameter
γ	Transverse shear strain
δ	Warping function parameter
ε	Strain
η, ζ	Local coordinates for laminate
λ	Torsional related warping
θ	Ply angle
σ	Stress
Φ	Twist angle
Ω	Rotational speed
$()_h$	Horizontal wall
$()_v$	Vertical wall

CHAPTER 1

1.1 Introduction

In recent years, composites are widely used in the aerospace industry and the robotic manufacturing industry due to a wide range of advantages – high strength to weight ratio, high stiffness, corrosive resistance and high fatigue resistance. The Boeing 787 Dreamliner uses 70% to 80% of composite materials as its structural components which is indicative of the importance of composite materials in the aircraft engineering applications. However, when these structures are exposed to elevated hydrothermal conditions, the efficiency of the structure may decrease, forcing the member to lower the allowable loading on it. Hence the study of these effects will allow structures to be designed with the capability of resisting environmental circumstances. Dynamic analysis of the structure under elevated temperature gradient is also very important along with static analysis for the aircraft structures design. Failure of most of the mechanical and structural systems can be associated with vibration. For aircrafts, structural failures are usually associated with vibration resulting in fatigue. In general, helicopter blades are made of composite materials due to their advantages as discussed previously. From Figure 1, it can be seen that the box-beam is the main structure which provides stiffness to the entire blade. Thus, it is important to study the dynamic behavior (vibration

characteristics) of these box-beams with the effect of environmental conditions on the structure.

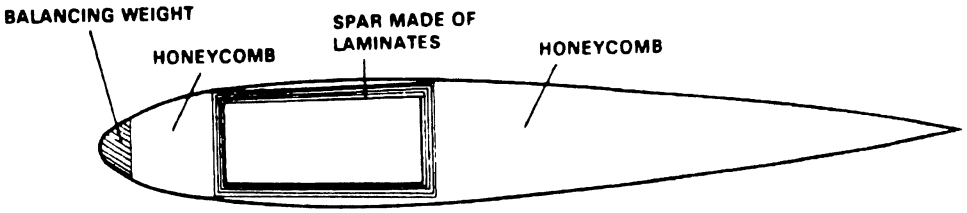

Figure 1: Composite blade assembly [4]

1.2 Literature Survey

There have been a number of literatures available conducted on findings the free vibration characteristics of a composite box beam. However, the thermal effects have been ignored. It is also important to include thermal effects in the analysis as composites are sensitive to temperature changes. There is only one paper [7] available that deals with thermal stresses but this paper deals with only static analysis.

Hodges and Dowell [1], initially focused on analytical derivation of the set of linear partial differential equations of motion for non-uniform helicopter blades describing the coupled bending and twisting nature. Houbolt and Brooks [2], discussed non-classical effects on the behavior of a composite box-beam such as bending and transverse shear coupling and torsional warping rigidity.

Hong and Chopra [3] and [4] proved that the aeroelastic performance of a helicopter rotor blade can be affected by controlling the laminate parameters ply angle and stacking sequence in their analysis. However, in this analysis, the effect of the direct

transverse shear is neglected and the effect of cross-sectional warping was assumed to depend only on the geometry of the beam cross-section.

Smith and Chopra [5], then improved the work done in Ref. [3] by including the direct transverse shear effects and shear stiffness in each wall. A direct analytical beam formulation was developed for predicting the elastic stiffness and the deformation behavior of the composite box-beam. This analysis is evaluated for a thin walled composite box-beam with no elastic coupling, but includes the extension-torsion and bending-shear couplings. In this analysis, they showed the importance of three non-classical structural phenomena - influence of torsion related out-of-plane warping on deformation, couplings associated with transverse shear deformation and the two-dimensional in-plane elastic behavior of the plies.

Chandra and Chopra [6] studied a theoretical and experimental analysis of free vibration characteristics of a thin walled rotating composite box-beam with bending-twist and extension-twist coupling. This model used a solid-section approach and contained transverse shear coupling and cross-sectional warping. The governing equations of motion are obtained using the Newtonian method. This analysis emphasized the influence of bending-shear coupling and extension-shear coupling o free vibration characteristics of thin walled composite box-beams with symmetric and anti-symmetric layup.

Anita and Chopra [7] developed an analytical method for predicting the effective thermal strains and load deformations of a composite box-beam. However this analysis only deals with the static behavior of the beam. They discussed the importance of thermal pre-twist of a composite box-beam for different ply configurations.

The main purposes of the current work is: (1) to develop a direct analytical method for generating the equations of motion for a thin-walled composite box-beam undergoing fixed axis rotation when subjected to a thermal environment by using the equations in Ref . [6], (2) to determine the free vibration solution of a thin walled cantilever composite box-beam with and without thermal effects, (3) to compare the results with previously published papers.

CHAPTER 2

Formulation of the Equations

2.1 Governing Equations of Motion for a Beam with Fixed Axis Rotation

The governing equations of motion are obtained for a long slender a thin-walled box-beam as shown in Figures 3-6. Following analysis was presented in Ref. [6], the governing equations are derived by using the D'Alembert's method and small deflection theory. Direct transverse shear can be neglected as its length to depth ratio is more than ten. However, the elastic coupling terms involving transverse shear have been retained. The corresponding moments and forces acting on the beam are shown in Figures 3-6

Using D'Alembert's approach, the equation of motion can be obtained by setting the summation of forces and summation of moments in x, y z direction to zero. These conditions yield the following equations:

$$for \sum M = 0$$

$$\frac{\partial M_x}{\partial x} + V_z \frac{\partial v}{\partial x} - V_y \frac{\partial w}{\partial x} + q_x = 0 \qquad (1)$$

$$\frac{\partial M_y}{\partial x} + V_z - V_x \frac{\partial w}{\partial x} + q_v = 0 \tag{2}$$

$$\frac{\partial M_z}{\partial x} + V_y - V_x \frac{\partial v}{\partial x} + q_z = 0 \tag{3}$$

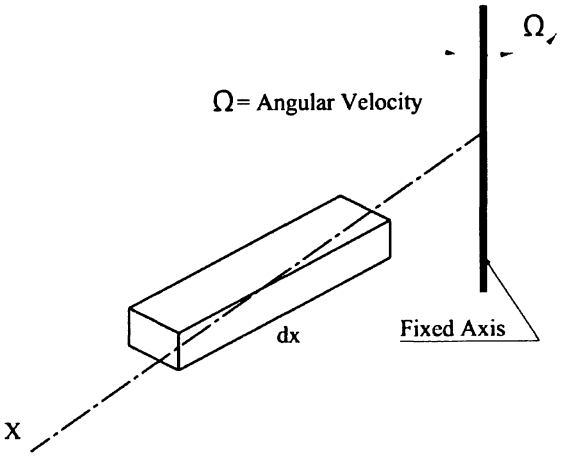

Figure 2: Fixed-axis rotation of the beam after deformation

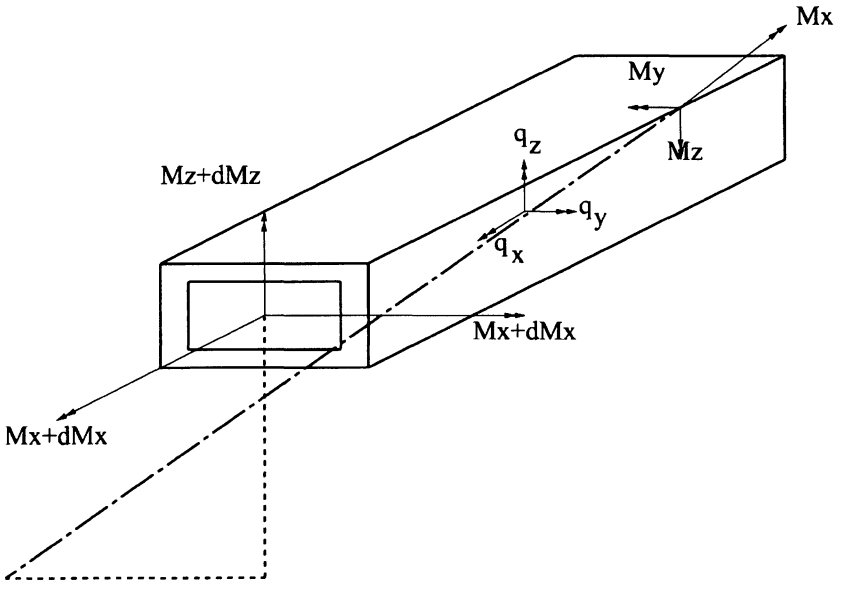

Figure 3: Box-beam with torsion, bending moments and inertial moments per length

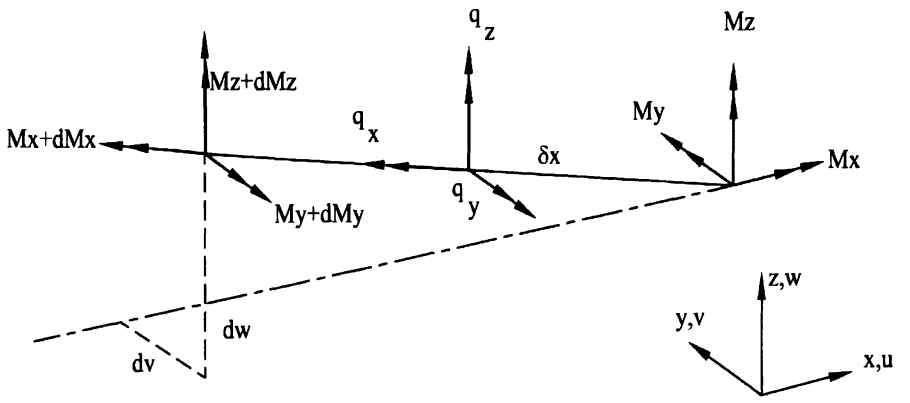

Figure 4: Line diagram of a box-beam with torsion, bending moments and inertial moments per length

$$for \sum F = 0$$

$$\frac{\partial V_x}{\partial x} + p_x = 0 \tag{4}$$

$$\frac{\partial V_y}{\partial x} + p_y = 0 \tag{5}$$

$$\frac{\partial V_z}{\partial x} + p_z = 0 \tag{6}$$

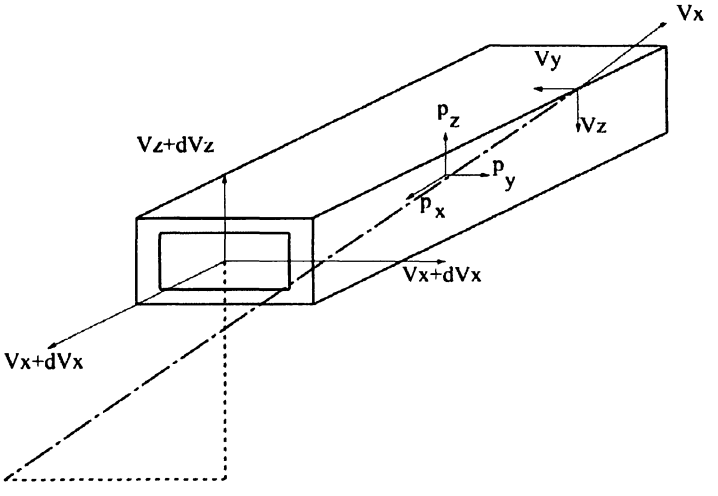

Figure 5: Box-beam with axial force, shear force and inertial forces per length

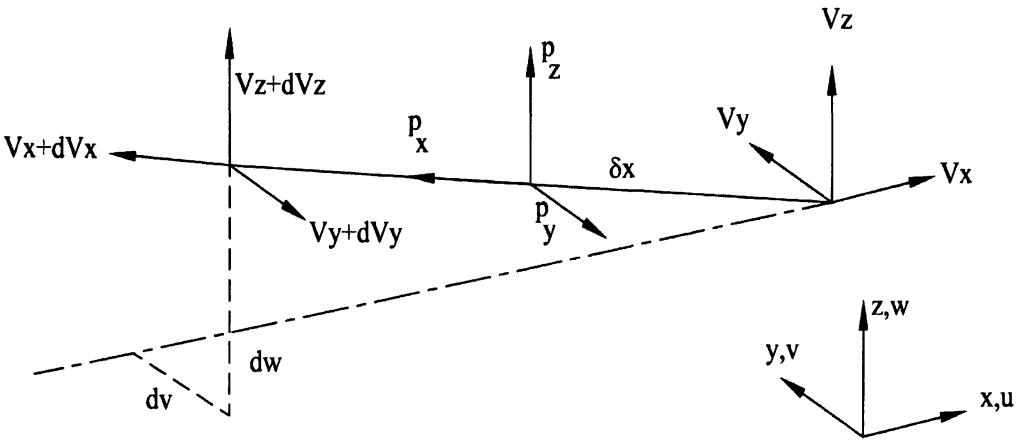

Figure 6: Line diagram of a box-beam with axial force, shear force and inertial forces per length

Where the inertial forces and moments in the beam are given below,

$$\begin{aligned} p_x &= m\Omega^2 x \\ p_y &= -m(v_{tt} - \Omega^2 v) \\ p_z &= m w_{tt} \end{aligned} \tag{7}$$

$$\begin{aligned} q_x &= -mK_m^2 \Phi_{tt} - \frac{1}{2} m\Omega^2 (K_{m2}^2 - K_{m1}^2) \sin 2\Phi \\ q_y &= 0 \\ q_z &= 0 \end{aligned} \tag{8}$$

Equations.(1)-(6) are simplified by eliminating the V_y and V_z to obtain the equation of motion for flap, lag, torsion and extension as follows.

From Eq. (2):

$$V_z = -\frac{\partial M_y}{\partial x} + V_x \frac{\partial w}{\partial x} - q_y \tag{9}$$

accidents attributed to aircraft malfunctions and environmental factors as the primary cause of the accident, with alcohol as the secondary contributory element, was also noticeable. The percentage of 'Other Factors' was comparable to 'Alcohol Involved' accidents in all the subdivisions of the groups. Flightcrew errors, also referred to as the 'Human factor' errors were almost two third of all accidents in both the groups. The percentage of Alcohol Involved, Flightcrew errors and Environmental factors exceeded the Other Factors group. The study clearly indicates the magnitude of Flightcrew related accidents in aviation. The data extracted from the study is depicted in the histogram below:

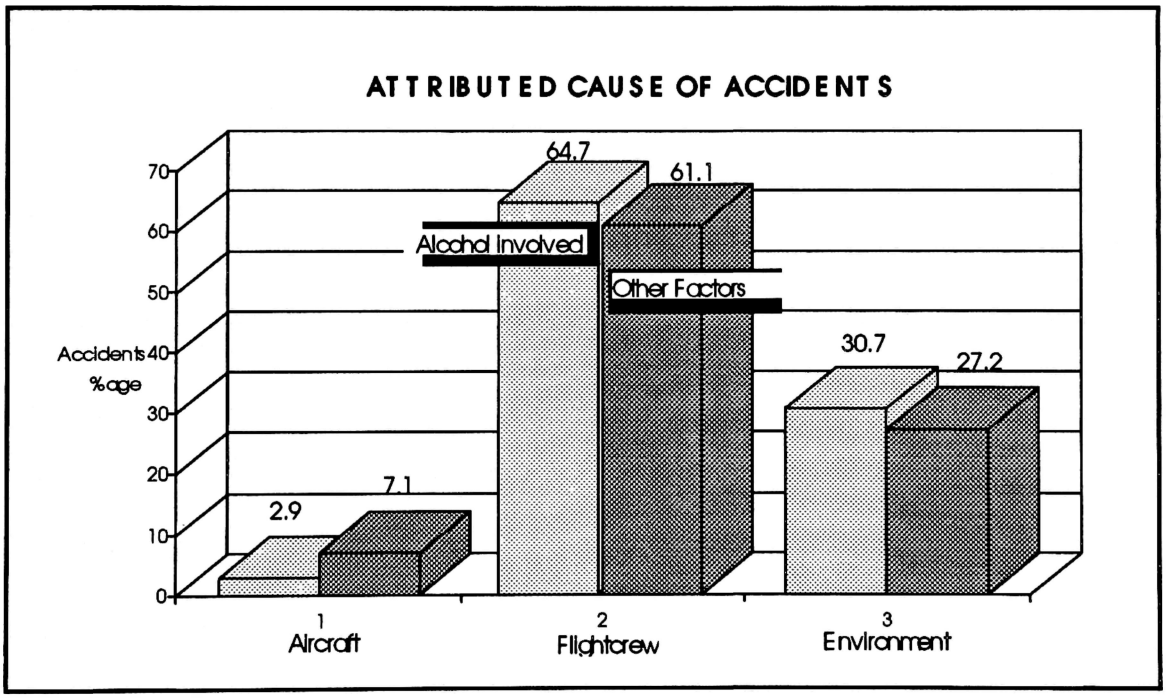

Figure 1. Data on Alcohol Related Accidents. Data Source: NTSB, Safety Study. October, 1992.

Extension

$$\frac{\partial V_x}{\partial x} + p_x = 0 \tag{16}$$

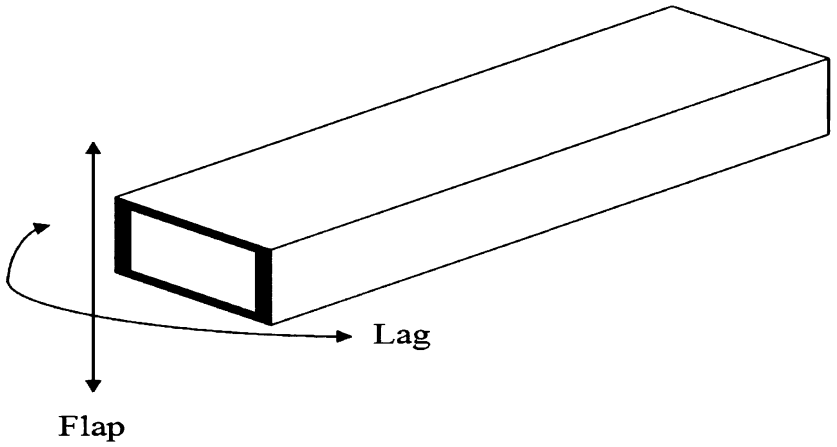

Figure 7: Flap-wise and lag-wise movement of a box-beam

From the analysis done by Smith and Chopra [6], the force displacement relations for a symmetric laminated composite box-beam are given by

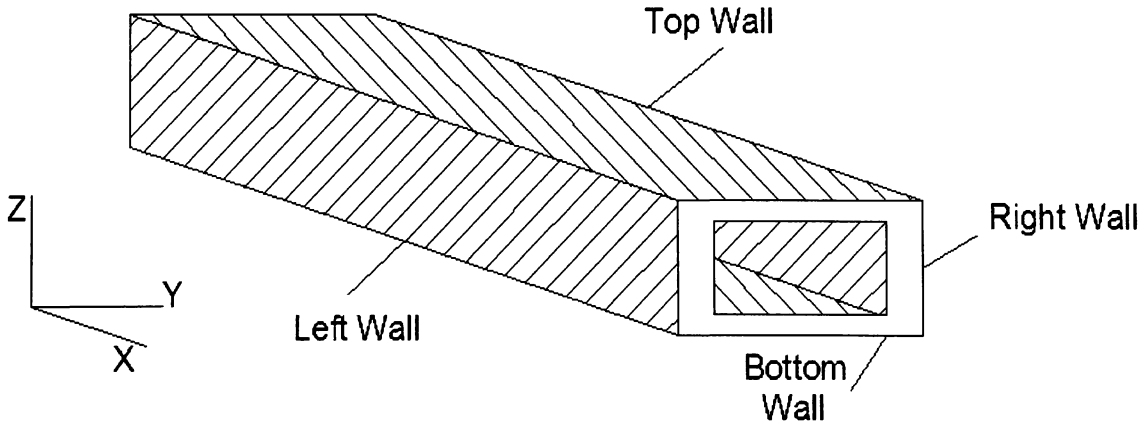

Figure 8: Symmetric box-beam

$$\begin{Bmatrix} V_x \\ V_y \\ V_z \end{Bmatrix} = \begin{bmatrix} K_{11} & K_{12} & K_{13} \\ K_{12} & K_{22} & 0 \\ K_{13} & 0 & K_{33} \end{bmatrix} \begin{Bmatrix} \varepsilon_{xx} \\ \varepsilon_{xy} \\ \varepsilon_{xz} \end{Bmatrix} \tag{17}$$

$$\begin{Bmatrix} M_x \\ M_y \\ M_z \end{Bmatrix} = \begin{bmatrix} K_{44} & K_{45} & K_{46} \\ K_{45} & K_{55} & 0 \\ K_{46} & 0 & K_{66} \end{bmatrix} \begin{Bmatrix} \phi_{,x} \\ w_{,xx} - \varepsilon_{xy\,,x} \\ v_{,xx} - \varepsilon_{xz\,,x} \end{Bmatrix} \tag{18}$$

Where $\varepsilon_{()} = \gamma^{o}_{()}$

Substituting the above relations into Eqs. (12)-(16) yields the equation of motion in the flap, lag and torsion directions for a thin walled symmetric composite box-beam.

Flap

$$K_{55}\frac{\partial^4 w}{\partial x^4} + K_{45}\frac{\partial^3 \Phi}{\partial x^3} + m\frac{\partial^2 w}{\partial t^2} - \frac{1}{2}m\Omega^2\frac{\partial}{\partial x}\left(\frac{\partial w}{\partial x}\left(l^2 - x^2\right)\right) = 0 \tag{19}$$

Lag

$$K_{66}\frac{\partial^4 v}{\partial x^4} + K_{46}\frac{\partial^3 \Phi}{\partial x^3} + m\frac{\partial^2 v}{\partial t^2} - m\Omega^2 v - \frac{1}{2}m\Omega^2\frac{\partial}{\partial x}\left(\frac{\partial v}{\partial x}\left(l^2 - x^2\right)\right) + m\Omega^2 K_{66} L_{22}\frac{\partial^2 v}{\partial x^2} = 0 \tag{20}$$

Torsion

$$K_{44}\frac{\partial^2 \Phi}{\partial x^2} + K_{45}\frac{\partial^3 w}{\partial x^3} + K_{46}\frac{\partial^3 v}{\partial x^3} - mK_m^2\frac{\partial^2 \Phi}{\partial t^2} - m\Omega^2\left(K_{m2}^2 - K_{m1}^2\right)\Phi + \frac{1}{2}m\Omega^2 K_A^2\frac{\partial}{\partial x}\left(\frac{\partial \Phi}{\partial x}\left(l^2 - x^2\right)\right) + m\Omega^2 K_{46} L_{22}\frac{\partial v}{\partial x} = 0 \tag{21}$$

2.2 Stiffness Matrix Formulation:

The stiffness matrix for a thin walled box beam was obtained by Smith and Chopra in Ref. [5]. In order to deal with the composite box beam, it is important to set the local coordinate system along with the global coordinate system, which is as shown Figures 9-10.

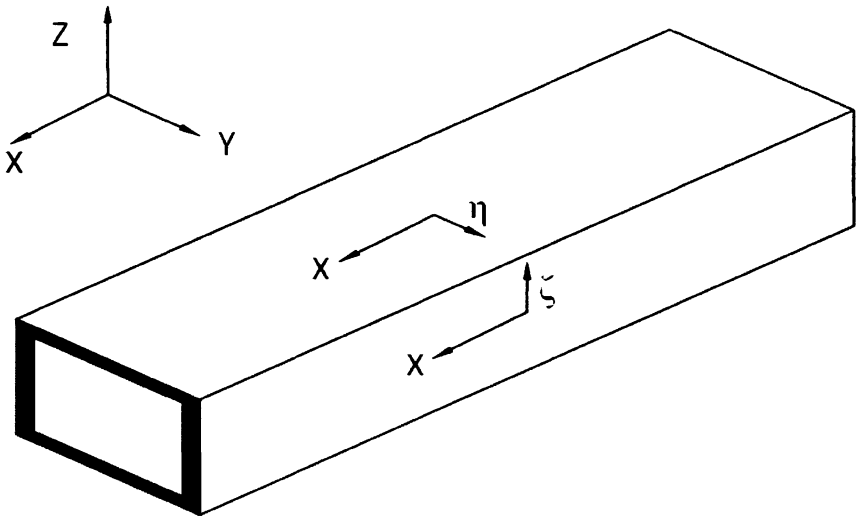

Figure 9: Box-beam with local and global co-ordinate system

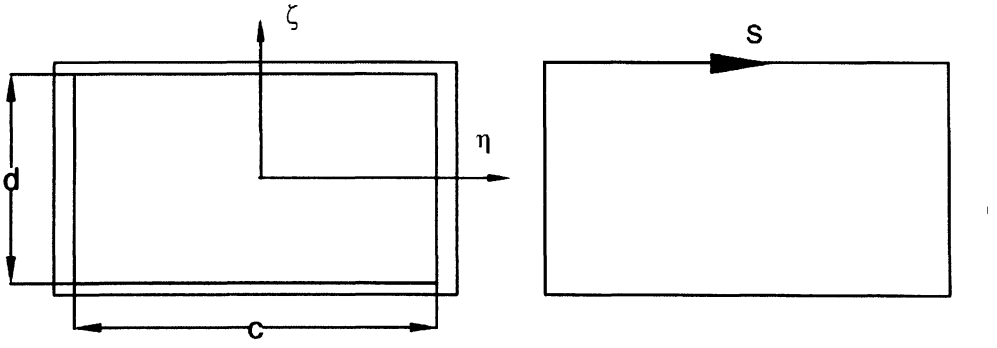

Figure 10: Box-beam cross-sectional dimensions and the contour

The stretching, bending, twisting, shearing and warping factors can be used to describe the total deformation of the beam cross section. These assumptions yield the following displacement functions [6].

$$U = u(x) - \eta\left[v'(x) - \gamma^0_{x\eta}(x)\right] - \zeta\left[w'(x) - \gamma^0_{x\zeta}(x)\right] - \underline{\lambda\phi'(x)} \tag{22}$$

$$V = v(x) - \zeta\phi(x) \tag{23}$$

$$W = w(x) + \eta\phi(x) \tag{24}$$

The underlined term in the Eq. (22) represents the warping, which is the out-of-plane axial displacement of the cross-section due to the torsion effect in the beam. The torsion-warping plays a key role in the analysis of a thin walled box beam as discussed in Ref. [10]-[13]. In the paper by Smith and Chopra [6], the warping deflections of a composite box beam are calculated by modifying the analysis done in Ref. [13] for a box-beam contour form of warping obtained as follows [5].

$$\lambda(s) = 2A\left(\frac{\delta_{os}}{\delta} - \frac{A_{os}}{A}\right) \tag{25}$$

Where, A is the enclosed area of the beam cross-section given by: $A = cd$

Other contour parameters are defined as

$$\delta = \int_s \frac{ds}{G(s)t(s)}$$
$$\delta_{os}(s) = \int_0^s \frac{ds}{G(s)t(s)} \tag{26}$$

Where A_{OS} is the swept area by the generator form s=0 to s=s on the contour surface. The generator starts at the box-beam center. On solving the Eq. (25), the contour warping function $\lambda(s)$, can be simply transformed into a two dimensional cross-section forms as given in Ref. [6].

$$\lambda(\eta,\zeta) = \beta\eta\zeta \tag{27}$$

Where, β is called warping constant, given by

$$\beta = -\left(\frac{1-\alpha}{1+\alpha}\right) \tag{28}$$

in which

$$\alpha = \left(\frac{c}{d}\right)\left(\frac{t_v}{t_h}\right)\left(\frac{G_v}{G_h}\right) \tag{29}$$

To compute the dimensionless warping constant (β), an effective in-plane shear stiffness for the composite beam walls must be specified. For this purpose each wall of the box-beam is considered to be a single laminated plate.

The in-plane stress and in-plane strain relations are as follows:

$$\begin{Bmatrix} N_{xx} \\ N_{yy} \\ N_{xy} \end{Bmatrix} = \begin{bmatrix} A_{11} & A_{12} & A_{16} \\ A_{12} & A_{22} & A_{26} \\ A_{16} & A_{26} & A_{66} \end{bmatrix} \begin{Bmatrix} \varepsilon_{xx} \\ \varepsilon_{yy} \\ \varepsilon_{xy} \end{Bmatrix} \tag{30}$$

Where,

$$A_{ij} = \sum_{n=1}^{number\ of\ plies} \overline{Q}_{ij}^{n}\, t_{ply}'' \tag{31}$$

The elements of the ply stiffness matrix $\overline{Q}_{ij}$ in the global coordinate system represent the macro-mechanical characteristics of the composite laminate, Ref. [8].

Assuming the in-plane transverse stress to be small for beam structures, i.e. N_{yy} can be neglected, and then the stiffness matrix can be simplified to

$$A' = \begin{bmatrix} \left(A_{11} - \frac{A_{12}^2}{A_{22}}\right) & \left(A_{16} - \frac{A_{12}A_{26}}{A_{22}}\right) \\ \left(A_{16} - \frac{A_{12}A_{26}}{A_{22}}\right) & \left(A_{11} - \frac{A_{26}^2}{A_{22}}\right) \end{bmatrix} \tag{32}$$

or

$$A' = \begin{bmatrix} A'_{11} & A'_{16} \\ A'_{16} & A'_{66} \end{bmatrix} \tag{33}$$

An in-plane effective shear modulus for a horizontal beam wall is defined by

$$G_{Effective,h} = \left(\frac{1}{t}\right)\left[A'_{66} - \left(\frac{A'^2_{16}}{A'_{11}}\right)\right] \tag{34}$$

A similar analysis can be applied to get the in-plane effective shear modulus for a vertical wall.

Strains can be calculated from the assumed displacement functions given by Eqs. (22) - (24). As we are dealing with a thin walled beam, only axial and in-plane shear strains are predominant. From classical mechanics the strain displacement relations are given by Eq. (35)

$$\varepsilon_{xx} = \frac{\partial U}{\partial x}$$
$$\varepsilon_{yy} = \frac{\partial V}{\partial y} \tag{35}$$
$$\varepsilon_{xy} = \frac{\partial U}{\partial y} + \frac{\partial V}{\partial x}$$

Substituting Eqs. (22) - (24) into Eq. (33) and solving we get,

$$\varepsilon_{xx} = u' - \eta\left(v'' - \gamma_{x\eta}^{0}{}'\right) - \zeta\left(w'' - \gamma_{x\zeta}^{0}{}'\right) - \lambda\phi''$$
$$\varepsilon_{x\zeta} = \left(\eta - \frac{\partial\lambda}{\partial\zeta}\right)\phi' + \gamma_{x\zeta}^{0}{}' \tag{36}$$

In the vertical walls and

$$\varepsilon_{xx} = u' - \eta\left(v'' - \gamma_{x\eta}^{0}{}'\right) - \zeta\left(w'' - \gamma_{x\zeta}^{0}{}'\right) - \lambda\phi''$$
$$\varepsilon_{x\eta} = -\left(\zeta + \frac{\partial\lambda}{\partial\eta}\right)\phi' + \gamma_{x\eta}^{0}{}' \tag{37}$$

In the horizontal wall

The elastic relations for the box-beam are

$$\begin{Bmatrix} \sigma_{xx} \\ \sigma_{yy} \\ \sigma_{xy} \end{Bmatrix} = \begin{bmatrix} \overline{Q_{11}} & \overline{Q_{12}} & \overline{Q_{16}} \\ \overline{Q_{12}} & \overline{Q_{22}} & \overline{Q_{26}} \\ \overline{Q_{16}} & \overline{Q_{26}} & \overline{Q_{66}} \end{bmatrix} \begin{Bmatrix} \varepsilon_{xx} \\ \varepsilon_{yy} \\ \varepsilon_{xy} \end{Bmatrix} \tag{38}$$

Equation. (36) can be applied to both the horizontal and vertical wall just by replacing the y with η and ζ, respectively.

The equilibrium condition for the beam requires that:

$$\iint_h \sigma_{\eta\eta} dA + \iint_v \sigma_{\zeta\zeta} dA = 0 \tag{39}$$

$$\iint_h \sigma_{\eta\eta} \zeta dA + \iint_v \sigma_{\zeta\zeta} \zeta dA = 0 \tag{40}$$

$$\iint_h \sigma_{\eta\eta} \eta dA + \iint_v \sigma_{\zeta\zeta} \eta dA = 0 \tag{41}$$

The transverse in-plane normal strain $\varepsilon_{\eta\eta}$ is determined to satisfy above condition. To specify $\varepsilon_{\eta\eta}$, it is necessary to assume it as a continuous function across the cross-section of the beam as.

$$\varepsilon_{yy} = au' + bv'' + cw'' + d\phi' + e\phi'' + f\gamma_{xy}^0 + g\gamma_{xz}^0 \tag{42}$$

The coefficients are assumed to be linear functions within the cross-section.

$$\begin{aligned} a &= a_0 + a_1\eta + a_2\zeta \\ b &= b_0 + b_1\eta + b_2\zeta \\ c &= c_0 + c_1\eta + c_2\zeta \end{aligned} \tag{43}$$

In which constants a_i, b_i, c_i, d_i, f_i and g_i can be calculated using Eqs. (39) – (41).

$$\iint_h \sigma_{\eta\eta} \eta dA + \iint_v \sigma_{\zeta\zeta} \eta dA = 0 \tag{44}$$

Plugging in the values of $\sigma_{\eta\eta}$ and $\sigma_{\zeta\zeta}$ in Eq. (44),

$$\iint_h \left(\overline{Q_{12}}\varepsilon_{xx} + \overline{Q_{22}}\varepsilon_{\eta\eta} + \overline{Q_{26}}\varepsilon_{x\eta}\right)\eta dA + \iint_v \left(\overline{Q_{12}}\varepsilon_{xx} + \overline{Q_{22}}\varepsilon_{\zeta\zeta} + \overline{Q_{26}}\varepsilon_{x\zeta}\right)\eta dA = 0 \tag{45}$$

$$\Rightarrow \begin{aligned} &\iint_h \left(\begin{aligned} &\overline{Q_{12}}\begin{bmatrix} u'-\eta\left(v''-\gamma^0_{x\eta}{}'\right) \\ -\zeta\left(w''-\gamma^0_{x\zeta}{}'\right)-\lambda\phi'' \end{bmatrix} + \overline{Q_{22}}\begin{bmatrix} au'+\{b_0+b_1\eta+b_2\zeta\}v''+ \\ cw''+d\phi'+e\phi''+f\gamma^0_{xy}+g\gamma^0_{xz} \end{bmatrix} \\ &+\overline{Q_{26}}\left[-\left(\zeta+\frac{\partial\lambda}{\partial\eta}\right)\phi'+\gamma^0_{x\eta}{}'\right] \end{aligned} \right)\eta dA + \\ &\iint_v \left(\begin{aligned} &\overline{Q_{12}}\begin{bmatrix} u'-\eta\left(v''-\gamma^0_{x\eta}{}'\right) \\ -\zeta\left(w''-\gamma^0_{x\zeta}{}'\right)-\lambda\phi'' \end{bmatrix} + \overline{Q_{22}}\begin{bmatrix} au'+\{b_0+b_1\eta+b_2\zeta\}v''+ \\ cw''+d\phi'+e\phi''+f\gamma^0_{xy}+g\gamma^0_{xz} \end{bmatrix} \\ &+\overline{Q_{26}}\left[\left(\eta-\frac{\partial\lambda}{\partial\zeta}\right)\phi'+\gamma^0_{x\zeta}{}'\right] \end{aligned} \right)\eta dA = 0 \end{aligned} \tag{46}$$

Examining the coefficients of v'' in the Eq. (46),

$$-\iint_{h,v}\overline{Q_{12}}\eta^2 dA + \iint_{h,v}\overline{Q_{22}}b_1\eta^2 dA = 0 \tag{47}$$

$$b_1 = \frac{\iint_{h,v}\overline{Q_{12}}\eta^2 dA}{\iint_{h,v}\overline{Q_{22}}\eta^2 dA} \tag{48}$$

The similar procedure can be followed to find the other constant values i.e. a_0, a_1, a_2, b_0, b_2, so on.

2.3 Thermal Effects

In practice, aircraft are subjected to changes in altitude depending upon the flying conditions, hence temperature gradient will be created; this generates thermal strains in the structure. This additional strain in the structure will affect the stability of the system. To make the structure dynamically stable it is important to study how the natural

frequency of the structure behaves under thermal strains. The relationship between thermal strain and temperature difference are given as follows:

$$\begin{aligned}\varepsilon_{xx}^{T} &= \alpha_{xx}\Delta T \\ \varepsilon_{yy}^{T} &= h\alpha_{yy}\Delta T \\ \varepsilon_{xy}^{T} &= \alpha_{xy}\Delta T\end{aligned} \tag{49}$$

Where h is the linear function within the cross-section

$$h = h_0 + h_1\eta + h_2\zeta \tag{50}$$

Equation. (49) can be applied to both the horizontal and vertical wall just by replacing the y with η and ζ, respectively.

The elastic relations for the box-beam are

$$\begin{Bmatrix}\sigma_{xx}^{T} \\ \sigma_{yy}^{T} \\ \sigma_{xy}^{T}\end{Bmatrix} = \begin{bmatrix}\overline{Q_{11}} & \overline{Q_{12}} & \overline{Q_{16}} \\ \overline{Q_{12}} & \overline{Q_{22}} & \overline{Q_{26}} \\ \overline{Q_{16}} & \overline{Q_{26}} & \overline{Q_{66}}\end{bmatrix}\begin{Bmatrix}\varepsilon_{xx}^{T} \\ \varepsilon_{yy}^{T} \\ \varepsilon_{xy}^{T}\end{Bmatrix} \tag{51}$$

or

$$\begin{aligned}\sigma_{xx}^{T} &= \overline{Q_{11}}\varepsilon_{xx}^{T} + \overline{Q_{12}}\varepsilon_{yy}^{T} + \overline{Q_{16}}\varepsilon_{xy}^{T} \\ \sigma_{yy}^{T} &= \overline{Q_{12}}\varepsilon_{xx}^{T} + \overline{Q_{22}}\varepsilon_{yy}^{T} + \overline{Q_{26}}\varepsilon_{xy}^{T} \\ \sigma_{xy}^{T} &= \overline{Q_{16}}\varepsilon_{xx}^{T} + \overline{Q_{26}}\varepsilon_{yy}^{T} + \overline{Q_{66}}\varepsilon_{xy}^{T}\end{aligned} \tag{52}$$

As throughout the analysis beam theory is used, as similar to the Eqs. (39) – (41), the net in-plane forces and the net in-plane moments due to the thermal effects should be zero.

$$\iint_h \sigma_{\eta\eta}^T dA + \iint_v \sigma_{\zeta\zeta}^T dA = 0 \tag{53}$$

$$\iint_h \sigma_{\eta\eta}^T \eta dA + \iint_v \sigma_{\zeta\zeta}^T \eta dA = 0 \tag{54}$$

$$\iint_h \sigma_{\eta\eta}^T \zeta dA + \iint_v \sigma_{\zeta\zeta}^T \zeta dA = 0 \tag{55}$$

Substituting Eq. (52) into Eq. (53) gives the h_0 value.

$$\iint_h \left(\overline{Q_{12}}\varepsilon_{xx}^T + \overline{Q_{22}}\varepsilon_{\eta\eta}^T + \overline{Q_{26}}\varepsilon_{x\eta}^T\right) dA + \iint_v \left(\overline{Q_{12}}\varepsilon_{xx}^T + \overline{Q_{22}}\varepsilon_{\zeta\zeta}^T + \overline{Q_{26}}\varepsilon_{x\zeta}^T\right) dA = 0 \tag{56}$$

$$\Rightarrow \iint_{h,v} \overline{Q_{12}}\varepsilon_{xx}^T dA + \iint_{h,v} \overline{Q_{22}}\varepsilon_{\zeta\zeta}^T dA + \iint_{h,v} \overline{Q_{26}}\varepsilon_{x\zeta}^T dA = 0 \tag{57}$$

Substituting Eq.49 in Eq.57,

$$\Rightarrow \iint_{h,v} \overline{Q_{12}}\left(\alpha_{xx}\Delta T\right) dA + \iint_{h,v} \overline{Q_{22}}\left[\left(h_0 + h_1\eta + h_2\zeta\right)\alpha_{yy}\Delta T\right] dA + \iint_{h,v} \overline{Q_{26}}\left(\alpha_{xy}\Delta T\right) dA = 0 \tag{58}$$

$$\Rightarrow \iint_{h,v} \overline{Q_{12}}\left(\alpha_{xx}\Delta T\right) dA + h_0 \iint_{h,v} \overline{Q_{22}}\left[\alpha_{yy}\Delta T\right] dA + \iint_{h,v} \overline{Q_{26}}\left(\alpha_{xy}\Delta T\right) dA = 0 \tag{59}$$

$$\Rightarrow h_0 = -\frac{\iint_{h,v} \overline{Q_{12}}\left(\alpha_{xx}\Delta T\right) dA + \iint_{h,v} \overline{Q_{26}}\left(\alpha_{xy}\Delta T\right) dA}{+\iint_{h,v} \overline{Q_{22}}\left[\alpha_{yy}\Delta T\right] dA} \tag{60}$$

$$h_0 = -\frac{\iint_{h,v} \overline{Q_{12}}\alpha_{xx}dA + \iint_{h,v} \overline{Q_{26}}\alpha_{xy}dA}{+\iint_{h,v} \overline{Q_{22}}\alpha_{yy}dA} \tag{61}$$

Substituting Eq. (52) into Eq. (54) and solving gives the h_1 value

$$\iint_h \left(\overline{Q_{12}}\varepsilon_{xx}^T\eta + \overline{Q_{22}}\varepsilon_{\eta\eta}^T\eta + \overline{Q_{26}}\varepsilon_{x\eta}^T\eta\right)dA + \iint_v \left(\overline{Q_{12}}\varepsilon_{xx}^T\eta + \overline{Q_{22}}\varepsilon_{\zeta\zeta}^T\eta + \overline{Q_{26}}\varepsilon_{x\zeta}^T\eta\right)dA = 0 \tag{62}$$

$$\Rightarrow \begin{array}{l} \iint_h \left(\overline{Q_{12}}\left(\alpha_{xx}\Delta T\right)\eta + \overline{Q_{22}}\left[\left(h_0 + h_1\eta + h_2\zeta\right)\alpha_{\eta\eta}\Delta T\right]\eta + \overline{Q_{26}}\left(\alpha_{x\eta}\Delta T\right)\eta\right)dA + \\ \iint_v \left(\overline{Q_{12}}\left(\alpha_{xx}\Delta T\right)\eta + \overline{Q_{22}}\left[\left(h_0 + h_1\eta + h_2\zeta\right)\alpha_{\zeta\zeta}\Delta T\right]\eta + \overline{Q_{26}}\left(\alpha_{x\zeta}\Delta T\right)\eta\right)dA = 0 \end{array} \tag{63}$$

$$\Rightarrow \iint_{h,v} \overline{Q_{22}}\left(h_1\eta^2\alpha_{yy}\right)dA = 0 \tag{64}$$

$$h_1 = 0 \tag{65}$$

Similarly, substituting Eq. (45) in Eq. (55) and solving gives

$$h_2 = 0 \tag{66}$$

Plugging in the values of h_1, h_2, h_0 in Eq. (49) results in ε_{yy}^T

$$\varepsilon_{yy}^T = \left(-\frac{\iint_{h,v} \overline{Q_{12}}\alpha_{xx}dA + \iint_{h,v} \overline{Q_{26}}\alpha_{xy}dA}{+\iint_{h,v} \overline{Q_{22}}\alpha_{yy}dA} \right)\alpha_{yy}\Delta T \tag{67}$$

Once the stress functions are obtained, it is easy to calculate the corresponding forces. Eq. (59) shows the relations between the force and the stress.

Axial load along the x-direction,

$$V_x^T = \iint_h \sigma_{xx}^T dA + \iint_v \sigma_{xx}^T dA \tag{68}$$

Substituting Eq. (52) in Eq. (68) yields,

$$\begin{aligned} V_x^T = & \iint_h \left[\overline{Q_{11}} \left(\alpha_{xx} \Delta T \right) + \overline{Q_{12}} \left(h_0 \alpha_{\eta\eta} \Delta T \right) + \overline{Q_{16}} \left(\alpha_{x\eta} \Delta T \right) \right] dA + \\ & \iint_v \left[\overline{Q_{11}} \left(\alpha_{xx} \Delta T \right) + \overline{Q_{12}} \left(h_0 \alpha_{\zeta\zeta} \Delta T \right) + \overline{Q_{16}} \left(\alpha_{x\zeta} \Delta T \right) \right] dA \end{aligned} \tag{69}$$

$$\Rightarrow V_x^T = \iint_{h,v} \left[\overline{Q_{11}} \alpha_{xx} \Delta T + \overline{Q_{12}} \left(h_0 \alpha_{yy} \Delta T \right) + \overline{Q_{16}} \left(\alpha_{xy} \Delta T \right) \right] dA \tag{70}$$

Shear load in y-direction,

$$V_y^T = \iint_v \left[\overline{Q_{12}} \varepsilon_{xx}^T + \overline{Q_{22}} \varepsilon_{yy}^T + \overline{Q_{26}} \varepsilon_{xy}^T \right] dA \tag{71}$$

Substituting Eq. (52) in Eq. (71) yields,

$$\Rightarrow V_y^T = \iint_h \left[\overline{Q_{16}} \left(\alpha_{xx} \Delta T \right) + \overline{Q_{26}} \left(h_0 \alpha_{\eta\eta} \Delta T \right) + \overline{Q_{66}} \left(\alpha_{x\eta} \Delta T \right) \right] dA \tag{72}$$

Shear load in z-direction,

$$V_z^T = \iint_v \left[\overline{Q_{12}} \varepsilon_{xx}^T + \overline{Q_{22}} \varepsilon_{yy}^T + \overline{Q_{26}} \varepsilon_{xy}^T \right] dA \tag{73}$$

Substituting Eq. (52) in Eq. (73) yields,

$$\Rightarrow V_z^T = \iint_v \left[\overline{Q_{16}} \left(\alpha_{xx} \Delta T \right) + \overline{Q_{26}} \left(h_0 \alpha_{\zeta\zeta} \Delta T \right) + \overline{Q_{66}} \left(\alpha_{x\zeta} \Delta T \right) \right] dA \tag{74}$$

Bending moment in y-direction,

$$M_y^T = \iint_h \sigma_{xx}^T \zeta \, dA \tag{75}$$

Substituting Eq. (52) in Eq. (75) yields,

$$\Rightarrow M_y^T = \iint_h \left[\overline{Q_{11}} \alpha_{xx} \Delta T \zeta + \overline{Q_{12}} \left(h_0 \alpha_{\eta\eta} \Delta T \right) \zeta + \overline{Q_{16}} \left(\alpha_{x\eta} \Delta T \right) \zeta \right] dA \tag{76}$$

Bending moment in z-direction,

$$M_z^T = \iint_v \sigma_{xx}^T \eta \, dA \tag{77}$$

Substituting Eq. (52) in Eq. (77) yields,

$$\Rightarrow M_z^T = \iint_v \left[\overline{Q_{11}} \alpha_{xx} \Delta T \eta + \overline{Q_{12}} \left(h_0 \alpha_{\zeta\zeta} \Delta T \right) \eta + \overline{Q_{16}} \left(\alpha_{x\zeta} \Delta T \right) \eta \right] dA \tag{78}$$

Torsion of the beam,

$$T^T = \iint \left[\left(\eta - \frac{\partial \lambda}{\partial \zeta} \right) \sigma_{x\zeta}^T - \left(\zeta + \frac{\partial \lambda}{\partial \eta} \right) \sigma_{x\eta}^T \right] dA \tag{79}$$

From Eq. (27),

$$\frac{\partial \lambda(\eta, \zeta)}{\partial \eta} = \beta \zeta \quad \text{and} \quad \frac{\partial \lambda(\eta, \zeta)}{\partial \zeta} = \beta \eta \tag{80}$$

Plugging Eq. (80) in Eq. (79),

$$T^T = \iint \left[(\eta - \beta \eta) \sigma_{x\zeta}^T - (\zeta + \beta \zeta) \sigma_{x\eta}^T \right] dA \tag{81}$$

Substituting Eq. (52) in Eq. (81) yields,

$$\Rightarrow \begin{aligned} T^T = & \iint_h \left\{(1-\beta)\left[\overline{Q_{16}}\left(\alpha_{xx}\Delta T\right)+\overline{Q_{26}}\left(h_0\alpha_{\zeta\zeta}\Delta T\right)+\overline{Q_{66}}\left(\alpha_{x\zeta}\Delta T\right)\right]\eta\right\} dA + \\ & \iint_v \left\{(1+\beta)\left[\overline{Q_{16}}\left(\alpha_{xx}\Delta T\right)+\overline{Q_{26}}\left(h_0\alpha_{\eta\eta}\Delta T\right)+\overline{Q_{66}}\left(\alpha_{x\eta}\Delta T\right)\right]\zeta\right\} dA \end{aligned} \tag{82}$$

From Eqs. (17)-(18) and Eqs. (70), (72), (76) and (78) we get

$$\begin{aligned} V_x = & \left[K_{11}\varepsilon_{xx}+K_{12}\varepsilon_{xy}+K_{13}\varepsilon_{xz}\right] \\ & + \iint_{h,v}\left[\overline{Q_{11}}\left(\alpha_{xx}\Delta T\right)+\overline{Q_{12}}\left(h_0\alpha_{yy}\Delta T\right)+\overline{Q_{16}}\left(\alpha_{xy}\Delta T\right)\right] dA \end{aligned} \tag{83}$$

$$\begin{aligned} M_x = & \left[K_{44}\phi_{,x}+K_{45}\left(w_{,xx}-\varepsilon_{xy,x}\right)+K_{13}\left(v_{,xx}-\varepsilon_{xz,x}\right)\right]+ \\ & \iint_h \left\{(1-\beta)\left[\overline{Q_{16}}\left(\alpha_{xx}\Delta T\right)+\overline{Q_{26}}\left(h_0\alpha_{\zeta\zeta}\Delta T\right)+\overline{Q_{66}}\left(\alpha_{x\zeta}\Delta T\right)\right]\eta\right\} dA + \\ & \iint_v \left\{(1+\beta)\left[\overline{Q_{16}}\left(\alpha_{xx}\Delta T\right)+\overline{Q_{26}}\left(h_0\alpha_{\eta\eta}\Delta T\right)+\overline{Q_{66}}\left(\alpha_{x\eta}\Delta T\right)\right]\zeta\right\} dA \end{aligned} \tag{84}$$

$$\begin{aligned} M_y = & \left[K_{45}\phi_{,x}+K_{55}\left(w_{,xx}-\varepsilon_{xy,x}\right)\right]- \\ & \iint_h \left[\overline{Q_{11}}\left(\alpha_{xx}\Delta T\right)\zeta+\overline{Q_{12}}\left(h_0\alpha_{\eta\eta}\Delta T\right)\zeta+\overline{Q_{16}}\left(\alpha_{x\eta}\Delta T\right)\zeta\right] dA \end{aligned} \tag{85}$$

$$\begin{aligned} M_z = & \left[K_{46}\phi_{,x}+K_{66}\left(v_{,xx}-\varepsilon_{xz,x}\right)\right]- \\ & \iint_v \left[\overline{Q_{11}}\left(\alpha_{xx}\Delta T\right)\eta+\overline{Q_{12}}\left(h_0\alpha_{\zeta\zeta}\Delta T\right)\eta+\overline{Q_{16}}\left(\alpha_{x\zeta}\Delta T\right)\eta\right] dA \end{aligned} \tag{86}$$

Substituting Eqs. (83) – (86) in the Eqs. (13) – (15) gives the equation of motion for a box-beam with thermal effects in the flap, lag and torsion directions when beam is rotating. These equations are as follows:

Flap – with rotation

$$K_{55}\frac{\partial^4 w}{\partial x^4}+K_{45}\frac{\partial^3 \Phi}{\partial x^3}+m\frac{\partial^2 w}{\partial t^2}- \frac{\partial}{\partial x}\left(\frac{\partial w}{\partial x}\left[\frac{1}{2}m\Omega^2\left(l^2-x^2\right)+\iint_{h,v}\left[\overline{Q_{11}}\alpha_{xx}\Delta T+\overline{Q_{12}}\left(h_0\alpha_{vv}\Delta T\right)+\overline{Q_{16}}\left(\alpha_{xv}\Delta T\right)\right]dA\right]\right)=0 \tag{87}$$

Lag – with rotation

$$K_{66}\frac{\partial^4 v}{\partial x^4}+K_{46}\frac{\partial^3 \Phi}{\partial x^3}+m\frac{\partial^2 v}{\partial t^2}-m\Omega^2 v- \frac{\partial}{\partial x}\left(\frac{\partial v}{\partial x}\left[\frac{1}{2}m\Omega^2\left(l^2-x^2\right)+\iint_{h,v}\left[\overline{Q_{11}}\alpha_{xx}\Delta T+\overline{Q_{12}}\left(h_0\alpha_{vy}\Delta T\right)+\overline{Q_{16}}\left(\alpha_{xy}\Delta T\right)\right]dA\right]\right) +m\Omega^2 K_{66}L_{22}\frac{\partial^2 v}{\partial x^2}=0 \tag{88}$$

Torsion – with rotation

$$K_{44}\frac{\partial^2 \Phi}{\partial x^2}+K_{45}\frac{\partial^3 w}{\partial x^3}+K_{46}\frac{\partial^3 v}{\partial x^3}-mK_m^2\frac{\partial^2 \Phi}{\partial t^2}-m\Omega^2\left(K_{m2}^2-K_{m1}^2\right)\Phi+ \frac{\partial}{\partial x}\left(\frac{\partial \Phi}{\partial x}\left[\frac{1}{2}m\Omega^2 K_A^2\left(l^2-x^2\right)+\iint_{h,v}\left[\overline{Q_{11}}\alpha_{xx}\Delta T+\overline{Q_{12}}\left(h_0\alpha_{yy}\Delta T\right)+\overline{Q_{16}}\left(\alpha_{xy}\Delta T\right)\right]dA\right]\right) +m\Omega^2 K_{46}L_{22}\frac{\partial v}{\partial x}=0 \tag{89}$$

Without rotation,

Flap – without rotation

$$K_{55}\frac{\partial^4 w}{\partial x^4}+K_{45}\frac{\partial^3 \Phi}{\partial x^3}+m\frac{\partial^2 w}{\partial t^2}- \left(\frac{\partial^2 w}{\partial x^2}\left[\iint_{h,v}\left[\overline{Q_{11}}\alpha_{xx}\Delta T+\overline{Q_{12}}\left(h_0\alpha_{yy}\Delta T\right)+\overline{Q_{16}}\left(\alpha_{xy}\Delta T\right)\right]dA\right]\right)=0 \tag{90}$$

Lag – without rotation

$$K_{66}\frac{\partial^4 v}{\partial x^4}+K_{46}\frac{\partial^3 \Phi}{\partial x^3}+m\frac{\partial^2 v}{\partial t^2}- \left(\frac{\partial^2 v}{\partial x^2}\left[\iint_{h,v}\left[\overline{Q_{11}}\alpha_{xx}\Delta T+\overline{Q_{12}}\left(h_0\alpha_{yy}\Delta T\right)+\overline{Q_{16}}\left(\alpha_{xy}\Delta T\right)\right]dA\right]\right)=0 \tag{91}$$

Torsion – without rotation

$$K_{44}\frac{\partial^2 \Phi}{\partial x^2}+K_{45}\frac{\partial^3 w}{\partial x^3}+K_{46}\frac{\partial^3 v}{\partial x^3}+ K_A^2\left(\frac{\partial^2 \Phi}{\partial x^2}\left[\iint_{h,v}\left[\overline{Q_{11}}\alpha_{xx}\Delta T+\overline{Q_{12}}\left(h_0\alpha_{yy}\Delta T\right)+\overline{Q_{16}}\left(\alpha_{xy}\Delta T\right)\right]dA\right]\right) -mK_m^2\frac{\partial^2 \Phi}{\partial t^2}=0 \tag{92}$$

Thus, Eqs. (90) - (92) are to be solved using the most reliable analytical technique to determine the natural frequency of the system.

CHAPTER 3

Method of Solution

3.1 Galerkin Method

This is the most widely used analytical technique in the engineering analysis. The solution of the Eigen-value problem is assumed in the form of a series of a comparison function which satisfy all the boundary conditions Ref.[9].

For example, let $R\left(\bar{\phi}, x\right)$ be a one-dimensional differential problem. This equation can be solved by assuming

$$\bar{\phi}_x^n = \sum_{i=1}^{n} c_i \phi_i(x)$$

Where, $\phi_i(x)$ is the admissible function and c_i is the coefficient to be determined.

According to this method, the admissible function is multiplied by the differential equation $R\left(\bar{\phi}, x\right)$, integrated over the domain of the system and set to zero.

$$\int_0^l R\left(\bar{\phi}'', x\right)\phi_i(x)\,dx = 0$$

Upon solving the above equations, a set of linear homogenous equations are obtained. The resulting equations are then solved for the Eigen-values and the unknown coefficients. A detailed analysis is given in Ref. [6].

3.2 Solution Procedure for a Cantilever Box-Beam

In this section the natural frequencies of a symmetric composite box-beam is determined. For this purpose a proper set of admissible functions are to be assumed such that they satisfy all the boundary conditions of the structure.

In general, the boundary conditions for a cantilever beam after neglecting the direct transverse shear [6] are

$$w=0,\quad v=0,\quad \phi=0,\quad w_x=0,\quad v_x=0 \tag{93}$$

The following functions are assumed to solve the problem using Galerkin's method:

$$w(x,t)=\sum_{i=1}^{n} a_i(t)\psi_i(x) \tag{94}$$

$$v(x,t)=\sum_{i=1}^{n} b_i(t)\psi_i(x) \tag{95}$$

$$\Phi(x,t)=\sum_{i=1}^{n} c_i(t)\sin\left(\frac{(2i-1)\pi}{2l}x\right) \tag{96}$$

Where,

l=length of the beam

$\psi_i(x)$ are the mode shapes of the beam.

For a cantilever beam $\psi_I(x)$ is given by

$$\psi_I(x) = \cosh\left(\frac{\lambda_I}{l}x\right) - \cos\left(\frac{\lambda_I}{l}x\right) - \alpha_I\left[\sinh\left(\frac{\lambda_I}{l}x\right) - \sin\left(\frac{\lambda_I}{l}x\right)\right]$$

3.3 Critical Temperature Difference (ΔT_{cr})

Before we start a discussion on the effect of temperature on the natural frequencies, it is important to find the critical temperature difference (ΔT_{cr}). Our equations are obtained based on the small deflection theory, thus we limited to pre-buckling solution only. If the temperature difference in the equation is varied more than the critical temperature difference the structure will no longer be in the linear state.

In the present analysis the critical temperature difference is determined by using Galerkin's method. In order to find ΔT_{cr}, we need to assume proper admissible functions for w, v and Φ, which are to be multiplied by flap, lag and torsion equations respectively and integrated over the beam length as discussed in the Sec.3.2.

For simplicity, the analysis for the non-rotating case is shown below. As the equations for rotating box-beam are tedious to do by hand, an appropriate computer program is generated to solve for the natural frequency.

Flap - without rotation

$$\int_0^l \left(K_{55}\frac{\partial^4 w}{\partial x^4} + K_{45}\frac{\partial^3 \Phi}{\partial x^3} - \left[\iint_{h,v} \left[\overline{Q_{11}}\alpha_{xx}\Delta T + \overline{Q_{12}}\left(h_0\alpha_{yy}\Delta T\right) + \overline{Q_{16}}\left(\alpha_{vy}\Delta T\right) \right] dA \right] \frac{\partial^2 w}{\partial x^2} + m\frac{\partial^2 w}{\partial t^2} \right) w_J(x)dx = 0 \qquad (97)$$

Lag - without rotation

$$\int_0^l \left(\begin{array}{l} K_{66}\dfrac{\partial^4 v}{\partial x^4} + K_{46}\dfrac{\partial^3 \Phi}{\partial x^3} + m\dfrac{\partial^2 v}{\partial t^2} \\ -\left[\iint_{h,v} \left[\overline{Q_{11}}\alpha_{xx}\Delta T + \overline{Q_{12}}\left(h_0\alpha_{yy}\Delta T\right) + \overline{Q_{16}}\left(\alpha_{xy}\Delta T\right) \right] dA \right] \dfrac{\partial^2 v}{\partial x^2} \end{array} \right) v_j(x)dx = 0 \qquad (98)$$

Torsion - without rotation

$$\int_0^l \left(\begin{array}{l} K_{44}\dfrac{\partial^2 \Phi}{\partial x^2} + K_{45}\dfrac{\partial^3 w}{\partial x^3} + K_{46}\dfrac{\partial^3 v}{\partial x^3} - mK_m^2\dfrac{\partial^2 \Phi}{\partial t^2} + \\ K_A^2\left(\dfrac{\partial^2 \Phi}{\partial x^2}\left[\iint_{h,v} \left[\overline{Q_{11}}\alpha_{xx}\Delta T + \overline{Q_{12}}\left(h_0\alpha_{yy}\Delta T\right) + \overline{Q_{16}}\left(\alpha_{xy}\Delta T\right) \right] dA \right] \right) \end{array} \right) \phi_j(x)dx = 0 \qquad (99)$$

As discussed in Section 3.1 for determination of critical temperature difference, Substituting in Eqs. (94) - (96) into Eqs. (97) - (99) and applying Galerkin's method to yield

Flap - without Rotation

$$\int_0^l \left(\begin{array}{l} K_{55}\dfrac{\partial^4 \sum_{i=1}^n a_i(t)\psi_i(x)}{\partial x^4} + K_{45}\dfrac{\partial^3 \sum_{i=1}^n c_i(t)\sin\left(\dfrac{(2i-1)\pi}{2l}x\right)}{\partial x^3} + m\dfrac{\partial^2 \sum_{i=1}^n a_i(t)\psi_i(x)}{\partial t^2} - \\ \left[\iint_{h,v} \left[\overline{Q_{11}}\alpha_{xx}\Delta T + \overline{Q_{12}}\left(h_0\alpha_{yy}\Delta T\right) + \overline{Q_{16}}\left(\alpha_{xy}\Delta T\right) \right] dA \right] \dfrac{\partial^2 \sum_{i=1}^n a_i(t)\psi_i(x)}{\partial x^2} \end{array} \right) \times \sum_{j=1}^n \psi_j(x)dx = 0 \qquad (100)$$

Lag - without rotation

$$\int_0^l \left(K_{66} \frac{\partial^4 \sum_{i=1}^{n} b_i(t)\psi_i(x)}{\partial x^4} + K_{46} \frac{\partial^3 \sum_{i=1}^{n} c_i(t) \sin\left(\frac{(2i-1)\pi}{2l} x\right)}{\partial x^3} + m \frac{\partial^2 \sum_{i=1}^{n} b_i(t)\psi_i(x)}{\partial t^2} - \left[\iint_{h,v} \left[\overline{Q_{11}} \alpha_{xx} \Delta T + \overline{Q_{12}} \left(h_0 \alpha_{yy} \Delta T \right) + \overline{Q_{16}} \left(\alpha_{xy} \Delta T \right) \right] dA \right] \frac{\partial^2 b_i(t)\psi_i(x)}{\partial x^2} \right) \times \sum_{j=1}^{n} \psi_j(x) dx = 0 \quad (101)$$

Torsion - without rotation

$$\int_0^l \left(K_{44} \frac{\partial^2 \sum_{i=1}^{n} c_i(t) \sin\left(\frac{(2i-1)\pi}{2l} x\right)}{\partial x^2} + K_{45} \frac{\partial^3 \sum_{i=1}^{n} a_i(t)\psi_i(x)}{\partial x^3} + K_{46} \frac{\partial^3 \sum_{i=1}^{n} b_i(t)\psi_i(x)}{\partial x^3} - mK_m^2 \frac{\partial^2 \sum_{i=1}^{n} c_i(t) \sin\left(\frac{(2i-1)\pi}{2l} x\right)}{\partial t^2} + K_A^2 \left(\frac{\partial^2 \sum_{i=1}^{n} c_i(t) \sin\left(\frac{(2i-1)\pi}{2l} x\right)}{\partial x^2} \left[\iint_{h,v} \left[\overline{Q_{11}} \alpha_{xx} \Delta T + \overline{Q_{12}} \left(h_0 \alpha_{yy} \Delta T \right) + \overline{Q_{16}} \left(\alpha_{xy} \Delta T \right) \right] dA \right] \right) \times \sum_{j=1}^{n} \sin\left(\frac{(2j-1)\pi}{2l} x\right) dx = 0 \quad (102)$$

Solving Eqs. (100) yields,

$$\int_0^l \left(\begin{array}{l} K_{55}\sum_{i=1}^{n}\sum_{j=1}^{m} a_i \left(\frac{\lambda_i}{l}\right)^4 \psi_i(x)\psi_j(x) + \\ \qquad K_{45}\sum_{i=1}^{n}\sum_{j=1}^{m} c_i \left(\frac{2i-1}{2l}\pi\right)^3 \cos\left(\frac{2i-1}{2l}\pi x\right)\psi_j(x) - \\ \left[\iint_{h,v} \left[\overline{Q_{11}}\alpha_{xx}\Delta T + \overline{Q_{12}}\left(h_0\alpha_{yy}\Delta T\right) + \overline{Q_{16}}\left(\alpha_{xy}\Delta T\right)\right] dA \right] \\ \qquad \times \sum_{i=1}^{n}\sum_{j=1}^{m} a_i \left(\frac{\lambda_i}{l}\right)^2 \psi_i(x)\psi_j(x) \end{array} \right) dx = 0 \tag{103}$$

Because of the importance of the first mode, only a first mode solution is used in this thesis. One can obtain this by taking only one term solution, i.e., i = 1 and j = 1 in the Eqs. (97) - (99)

$$\Rightarrow \begin{array}{l} K_{55}a_1\underline{\left(\frac{\lambda_1}{l}\right)^4} - K_{45}\int_0^l \left(c_1\left(\frac{1}{2l}\pi\right)^3 \cos\left(\frac{1}{2l}\pi x\right)\psi_1(x)\right) dx - \\ \qquad \left[\iint_{h,v} \left[\overline{Q_{11}}\alpha_{xx}\Delta T + \overline{Q_{12}}\left(h_0\alpha_{yy}\Delta T\right) + \overline{Q_{16}}\left(\alpha_{xy}\Delta T\right)\right] dA \right] a_1\left(\frac{\lambda_1}{l}\right)^2 = 0 \end{array} \tag{104}$$

$$\Rightarrow \begin{array}{l} a_1\left(\frac{\lambda_1}{l}\right)^2 \left(K_{55}\left(\frac{\lambda_1}{l}\right)^2 - \left[\iint_{h,v} \left[\overline{Q_{11}}\alpha_{xx}\Delta T + \overline{Q_{12}}\left(h_0\alpha_{yy}\Delta T\right) + \overline{Q_{16}}\left(\alpha_{xy}\Delta T\right)\right] dA \right] \right) \\ \qquad - c_1 K_{45}\left(\frac{1}{2l}\pi\right)^3 \int_0^l \left(\cos\left(\frac{1}{2l}\pi x\right)\psi_1(x)\right) dx = 0 \end{array} \tag{105}$$

Similarly solving the lag and torsion equation yields,

Lag - without rotation

$$K_{66}b_1\left(\frac{\lambda_1}{l}\right)^4+K_{46}\int_0^l\left(c_1\left(\frac{1}{2l}\pi\right)^3\cos\left(\frac{1}{2l}\pi x\right)\psi_1(x)\right)dx+$$
$$-\left[\iint_{h,v}\left[\overline{Q_{11}}\alpha_{xx}\Delta T+\overline{Q_{12}}\left(h_0\alpha_{yy}\Delta T\right)+\overline{Q_{16}}\left(\alpha_{xy}\Delta T\right)\right]dA\right]b_1\left(\frac{\lambda_1}{l}\right)^2=0 \tag{106}$$

$$\Rightarrow \quad b_1\left(\frac{\lambda_1}{l}\right)^2\left(K_{66}\left(\frac{\lambda_1}{l}\right)^2-\left[\iint_{h,v}\left[\overline{Q_{11}}\alpha_{xx}\Delta T+\overline{Q_{12}}\left(h_0\alpha_{yy}\Delta T\right)+\overline{Q_{16}}\left(\alpha_{xy}\Delta T\right)\right]dA\right]\right)+$$
$$c_1K_{46}\left(\frac{1}{2l}\pi\right)^3\int_0^l\left(\cos\left(\frac{1}{2l}\pi x\right)\psi_1(x)\right)dx=0 \tag{107}$$

Torsion - without rotation

$$K_{44}\int_0^l c_t(t)\sin\left(\frac{\pi}{2l}x\right)\sin\left(\frac{\pi}{2l}x\right)dx+K_{45}\int_0^l a_t(t)\left(\frac{\lambda_t}{l}\right)^3\psi_t(x)\sin\left(\frac{\pi}{2l}x\right)dx+$$
$$K_{46}\int_0^l b_t(t)\left(\frac{\lambda_t}{l}\right)^3\psi_t(x)\sin\left(\frac{\pi}{2l}x\right)dx+$$
$$K_A^2\left(\int_0^l c_t(t)\sin\left(\frac{\pi}{2l}x\right)\sin\left(\frac{\pi}{2l}x\right)dx\left[\iint_{h,v}\left[\begin{array}{l}\overline{Q_{11}}\alpha_{xx}\Delta T+\overline{Q_{12}}\left(h_0\alpha_{yy}\Delta T\right)\\+\overline{Q_{16}}\left(\alpha_{xy}\Delta T\right)\end{array}\right]dA\right]\right)=0 \tag{108}$$

$$a_1\left(\frac{\lambda_1}{l}\right)^3K_{45}\int_0^l\psi_1(x)\sin\left(\frac{\pi}{2l}x\right)dx+b_1\left(\frac{\lambda_1}{l}\right)^3K_{46}\int_0^l\psi_1(x)\sin\left(\frac{\pi}{2l}x\right)dx+$$
$$\Rightarrow \quad c_1\left\{K_{44}\frac{l}{2}+K_A^2\left(\frac{l}{2}\left[\iint_{h,v}\left[\begin{array}{l}\overline{Q_{11}}\alpha_{xx}\Delta T+\overline{Q_{12}}\left(h_0\alpha_{yy}\Delta T\right)\\+\overline{Q_{16}}\left(\alpha_{xy}\Delta T\right)\end{array}\right]dA\right]\right)\right\}=0 \tag{109}$$

Therefore Eqs. (105), (107), (109) can be written as

$$f_1 * a_1 + f_2 * b_1 + f_3 * c_1 = 0 \tag{110}$$

$$l_1 * a_1 + l_2 * b_1 + l_3 * c_1 = 0 \tag{111}$$

$$t_1 * a_1 + t_2 * b_1 + t_3 * c_1 = 0 \tag{112}$$

Where,

$$f_1 = \left(\frac{\lambda_1}{l}\right)^2 \left(K_{55} \left(\frac{\lambda_1}{l}\right)^2 - \left[\iint_{h,v} \left[\overline{Q_{11}} \alpha_{xx} \Delta T + \overline{Q_{12}} \left(h_0 \alpha_{yy} \Delta T \right) + \overline{Q_{16}} \left(\alpha_{xy} \Delta T \right) \right] dA \right] \right)$$

$$f_2 = 0$$

$$f_3 = K_{45} \left(\frac{1}{2l}\pi\right)^3 \int_0^l \left(\cos\left(\frac{1}{2l}\pi x\right) \psi_1(x) \right) dx$$

$$l_1 = 0$$

$$l_2 = \left(\frac{\lambda_1}{l}\right)^2 \left(K_{66} \left(\frac{\lambda_1}{l}\right)^2 - \left[\iint_{h,v} \left[\overline{Q_{11}} \alpha_{xx} \Delta T + \overline{Q_{12}} \left(h_0 \alpha_{yy} \Delta T \right) + \overline{Q_{16}} \left(\alpha_{xy} \Delta T \right) \right] dA \right] \right)$$

$$l_3 = K_{46} \left(\frac{1}{2l}\pi\right)^3 \int_0^l \left(\cos\left(\frac{1}{2l}\pi x\right) \psi_1(x) \right) dx$$

$$t_1 = \left(\frac{\lambda_1}{l}\right)^3 K_{45} \int_0^l \psi_1(x) \sin\left(\frac{\pi}{2l} x\right) dx$$

$$t_2 = \left(\frac{\lambda_1}{l}\right)^3 K_{46} \int_0^l \psi_1(x) \sin\left(\frac{\pi}{2l}x\right) dx$$

$$t_3 = K_{44}\frac{l}{2} + K_A^2\left(\frac{l}{2}\left[\iint_{h,\lambda}\left[\begin{array}{l}\overline{Q_{11}}\alpha_{xx}\Delta T + \overline{Q_{12}}\left(h_0\alpha_{yy}\Delta T\right) \\ +\overline{Q_{16}}\left(\alpha_{xy}\Delta T\right)\end{array}\right] dA\right]\right)$$

Putting Eqs. (110) - (112) in matrix form yields

$$\begin{pmatrix} f_1 & f_2 & f_3 \\ l_1 & l_2 & l_3 \\ t_1 & t_2 & t_3 \end{pmatrix}\begin{bmatrix} a_1 \\ b_1 \\ c_1 \end{bmatrix} = \begin{Bmatrix} 0 \\ 0 \\ 0 \end{Bmatrix} \tag{113}$$

For the nontrivial solution we set the determinant of the coefficients to zero in order to determine the critical temperature change, ΔT_{cr}

$$\begin{vmatrix} f_1 & f_2 & f_3 \\ l_1 & l_2 & l_3 \\ t_1 & t_2 & t_3 \end{vmatrix} = 0 \tag{114}$$

The underlined term in Eq. (104) can be found from the characteristic equation of a cantilever beam. In general it is

$$\cos\lambda l \cosh\lambda l + 1 = 0$$

Solving the above equation yields the n modes of Eigen-values, as follows

$\lambda_1 l = 1.8751$
$\lambda_2 l = 4.6941$
$\lambda_3 l = 7.8548$
$\vdots$
$\lambda_n l = \ldots$

3.4 Solving for Natural Frequency

As discussed in the Section 3.2 once the critical temperature difference is obtained, the temperature difference in the Eqs. (90) - (92) can be varied such that $\Delta T \le \Delta T_{cr}$.

Flap – without rotation

$$\int_0^l \left(K_{55} \frac{\partial^4 \sum_{i=1}^{n} a_i(t)\psi_i(x)}{\partial x^4} + K_{45} \frac{\partial^3 \sum_{i=1}^{n} c_i(t) \sin\left(\frac{(2i-1)\pi}{2l} x\right)}{\partial x^3} + m \frac{\partial^2 \sum_{i=1}^{n} a_i(t)\psi_i(x)}{\partial t^2} - \left[\iint_{h,v} \left[\overline{Q_{11}} \alpha_{xx} \Delta T + \overline{Q_{12}} \left(h_0 \alpha_{vv} \Delta T \right) + \overline{Q_{16}} \left(\alpha_{xy} \Delta T \right) \right] dA \right] \frac{\partial^2 \sum_{i=1}^{n} a_i(t)\psi_i(x)}{\partial x^2} \right) \times \sum_{j=1}^{n} \psi_j(x) dx = 0 \quad (115)$$

Lag – without rotation

$$\int_0^l \left(K_{66} \frac{\partial^4 \sum_{i=1}^{n} b_i(t)\psi_i(x)}{\partial x^4} + K_{46} \frac{\partial^3 \sum_{i=1}^{n} c_i(t) \sin\left(\frac{(2i-1)\pi}{2l} x\right)}{\partial x^3} + m \frac{\partial^2 \sum_{i=1}^{n} b_i(t)\psi_i(x)}{\partial t^2} - \left[\iint_{h,v} \left[\overline{Q_{11}} \alpha_{xx} \Delta T + \overline{Q_{12}} \left(h_0 \alpha_{vv} \Delta T \right) + \overline{Q_{16}} \left(\alpha_{xy} \Delta T \right) \right] dA \right] \frac{\partial^2 b_i(t)\psi_i(x)}{\partial x^2} \right) \times \sum_{j=1}^{n} \psi_j(x) dx = 0 \quad (116)$$

Torsion – without rotation

$$\int_0^l \left(\begin{array}{l} K_{44} \dfrac{\partial^2 \sum_{i=1}^{n} c_i(t) \sin\left(\dfrac{(2i-1)\pi}{2l} x\right)}{\partial x^2} + K_{45} \dfrac{\partial^3 \sum_{i=1}^{n} a_i(t)\psi_i(x)}{\partial x^3} + \\ K_{46} \dfrac{\partial^3 \sum_{i=1}^{n} b_i(t)\psi_i(x)}{\partial x^3} - mK_m^2 \dfrac{\partial^2 \sum_{i=1}^{n} c_i(t) \sin\left(\dfrac{(2i-1)\pi}{2l} x\right)}{\partial t^2} + \\ K_A^2 \left(\dfrac{\partial^2 \sum_{i=1}^{n} c_i(t) \sin\left(\dfrac{(2i-1)\pi}{2l} x\right)}{\partial x^2} \left[\iint_{h,v} \left[\begin{array}{l} \overline{Q_{11}} \alpha_{xx} \Delta T + \overline{Q_{12}} \left(h_0 \alpha_{yy} \Delta T \right) \\ + \overline{Q_{16}} \left(\alpha_{xy} \Delta T \right) \end{array} \right] dA \right] \right) \\ \times \sum_{j=1}^{n} \sin\left(\dfrac{(2j-1)\pi}{2l} x\right) dx = 0 \end{array} \right) \tag{117}$$

Solving Eq. (115),

$$\int_0^l \left(\begin{array}{l} K_{55} \sum_{i=1}^{n} \sum_{j=1}^{m} a_i \left(\dfrac{\lambda_i}{l}\right)^4 \psi_i(x)\psi_j(x) + \\ K_{45} \sum_{i=1}^{n} \sum_{j=1}^{m} c_i \left(\dfrac{2i-1}{2l}\pi\right)^3 \cos\left(\dfrac{2i-1}{2l}\pi x\right)\psi_j(x) + \\ m\ddot{a}_i \sum_{i=1}^{n} \sum_{j=1}^{m} \psi_i(x)\psi_j(x) - \\ \left[\iint_{h,v} \left[\overline{Q_{11}} \alpha_{xx} \Delta T + \overline{Q_{12}} \left(h_0 \alpha_{yy} \Delta T \right) + \overline{Q_{16}} \left(\alpha_{vv} \Delta T \right) \right] dA \right] \\ \times \sum_{i=1}^{n} \sum_{j=1}^{m} a_i \left(\dfrac{\lambda_i}{l}\right)^2 \psi_i(x)\psi_j(x) \end{array} \right) dx = 0 \tag{118}$$

For the first mode solution, we consider i = 1 and j=1 only

$$K_{55}a_1\underline{\left(\frac{\lambda_1}{l}\right)^4} - K_{45}\int_0^l\left(c_1\left(\frac{1}{2l}\pi\right)^3\cos\left(\frac{1}{2l}\pi x\right)\psi_1(x)\right)dx + m\ddot{a}_1\int_0^l\sum_{i=1}^{n}\sum_{j=1}^{m}\psi_i(x)\psi_j(x) - \left[\iint_{h,v}\left[\overline{Q_{11}}\alpha_{xx}\Delta T + \overline{Q_{12}}\left(h_0\alpha_{yy}\Delta T\right) + \overline{Q_{16}}\left(\alpha_{xy}\Delta T\right)\right]dA\right]a_1\left(\frac{\lambda_1}{l}\right)^2 = 0 \quad (119)$$

$$f_{m1}\ddot{a}_1 + f_{m2}a_1 + f_{m3}c_1 = 0 \quad (120)$$

Where,

$$f_{m1} = m\int_0^l\sum_{i=1}^{n}\sum_{j=1}^{m}\psi_i(x)\psi_j(x)$$

$$f_{m2} = K_{55}\left(\frac{\lambda_1}{l}\right)^4 - \left[\iint_{h,v}\left[\overline{Q_{11}}\alpha_{xx}\Delta T + \overline{Q_{12}}\left(h_0\alpha_{yy}\Delta T\right) + \overline{Q_{16}}\left(\alpha_{xy}\Delta T\right)\right]dA\right]\left(\frac{\lambda_1}{l}\right)^2$$

$$f_{m3} = -K_{45}\int_0^l\left(c_1\left(\frac{1}{2l}\pi\right)^3\cos\left(\frac{1}{2l}\pi x\right)\psi_1(x)\right)dx$$

Similar solving lag and torsion equations yield,

$$l_{m1}\ddot{b}_1 + l_{m2}b_1 + l_{m3}c_1 = 0 \quad (121)$$

$$t_{m1}\ddot{c}_1 + t_{m2}a_1 + t_{m3}b_1 + t_{m3}c_1 = 0 \quad (122)$$

Where,

$$l_{m1} = m\int_0^l \sum_{i=1}^{n}\sum_{j=1}^{m} \psi_i(x)\psi_j(x)$$

$$l_{m2} = K_{66}\left(\frac{\lambda_1}{l}\right)^4 - \left[\iint_{h,v}\left[\overline{Q_{11}}\alpha_{xx}\Delta T + \overline{Q_{12}}\left(h_0\alpha_{yy}\Delta T\right) + \overline{Q_{16}}\left(\alpha_{xy}\Delta T\right)\right]dA\right]\left(\frac{\lambda_1}{l}\right)^2$$

$$l_{m3} = -K_{46}\left(\frac{1}{2l}\pi\right)^3 \int_0^l \left(\cos\left(\frac{1}{2l}\pi x\right)\psi_1(x)\right)dx$$

$$t_{m1} = -mK_m^2\int_0^l \sum_{i=1}^{n}\sum_{j=1}^{m} \sin\left(\frac{(2i-1)\pi}{2l}x\right)\sin\left(\frac{(2j-1)\pi}{2l}x\right)dx$$

$$t_{m2} = \left(\frac{\lambda_1}{l}\right)^3 K_{45}\int_0^l \psi_1(x)\sin\left(\frac{\pi}{2l}x\right)dx$$

$$t_{m3} = \left(\frac{\lambda_1}{l}\right)^3 K_{46}\int_0^l \psi_1(x)\sin\left(\frac{\pi}{2l}x\right)dx$$

$$t_{m4} = \left\{K_{44}\frac{l}{2} + K_A^2\left(\frac{l}{2}\left[\iint_{h,v}\left[\begin{array}{l}\overline{Q_{11}}\alpha_{xx}\Delta T + \overline{Q_{12}}\left(h_0\alpha_{yy}\Delta T\right)\\ +\overline{Q_{16}}\left(\alpha_{xy}\Delta T\right)\end{array}\right]dA\right]\right)\right\}$$

Let the solution for the time dependent function be in exponential form, given as

$$\begin{aligned} a_1(t) &= ae^{\omega x}\\ b_1(t) &= be^{\omega x}\\ c_1(t) &= ce^{\omega x}\end{aligned} \qquad (123)$$

Differentiating Eq. (123) twice with respect to time yields

$$\begin{aligned} \ddot{a}_1(t) &= a\omega^2 e^{\omega x}\\ \ddot{b}_1(t) &= b\omega^2 e^{\omega x}\\ \ddot{c}_1(t) &= c\omega^2 e^{\omega x}\end{aligned} \qquad (124)$$

Substituting Eqs. (124) into Eqs. (120), (121), (122) and solving for the first mode solution yields

$$\left(f_{m1}\omega^2 + f_{m2}\right)ae^{\omega x} + f_{m3}ce^{\omega x} = 0 \tag{125}$$

$$\left(l_{m1}\omega^2 + l_{m2}\right)ae^{\omega x} + l_{m3}ce^{\omega x} = 0 \tag{126}$$

$$\left(t_{m1}\omega^2 + t_{m4}\right)ce^{\omega x} + t_{m2}ae^{\omega x} + t_{m3}be^{\omega x} = 0 \tag{127}$$

Putting Eqs. (125) - (127) in matrix form

$$\begin{pmatrix} \left(f_{m1}\omega^2 - f_{m2}\right) & 0 & f_{m3} \\ 0 & \left(l_{m1}\omega^2 - l_{m2}\right) & l_{m3} \\ t_{m3} & t_{m3} & \left(t_{m1}\omega^2 - t_{m4}\right) \end{pmatrix} \begin{bmatrix} a \\ b \\ c \end{bmatrix} e^{\omega x} = \begin{Bmatrix} 0 \\ 0 \\ 0 \end{Bmatrix} \tag{128}$$

For a non-trivial solution

$$\begin{vmatrix} \left(f_{m1}\omega^2 - f_{m2}\right) & 0 & f_{m3} \\ 0 & \left(l_{m1}\omega^2 - l_{m2}\right) & l_{m3} \\ t_{m3} & t_{m3} & \left(t_{m1}\omega^2 - t_{m4}\right) \end{vmatrix} = 0 \tag{129}$$

Solving the above determinant yields the natural frequency of the system in the flap and lag directions.

CHAPTER 4

Numerical Solution

4.1 Beam Geometric Configuration and Material Properties

To validate the analysis, Glass-Epoxy and Kevlar-Epoxy composite box beams are used as given in Ref. [6] and [14]. The geometric and material properties of the beam are given in Tables 1-2.

Material	E_L 10^6 psi	E_T 10^6 psi	G_{LT} 10^6 psi	υ	α_L 10^{-6} in/in/^{O}F	α_T 10^{-6} in/in/^{O}F	Mass Density 10^{-3}
Glass-Epoxy	7	2.1	0.8	0.26	4.77	12.278	0.1676
Kevlar-Epoxy	11	0.8	0.34	0.34	-1.1	3.3	0.1402

Table 1: Material properties used in the numerical evaluation of the analysis [6][14]

Beam Material	Number of plies	Ply thickness, in	Inner dimension of cross-section, $c \times d$ in^2	Ply angles		Length of beam, in
				Top and bottom	Left and right	
Glass-Epoxy	2	0.016	0.893 x 0.477	[45/45]	[45/-45]	33.25
Kevlar-Epoxy	2	0.010	0.893 x 0.477	[45/45]	[45/-45]	33.25

Table 2: Geometric properties for the box-beam used in this analysis [6]

4.2 Beam Stiffness Matrix

The stiffness matrices of the composite box-beam is determined by substituting in the material and geometric parameters in the MATLAB code developed in Appendix-A this thesis.

For Glass-Epoxy box-beam,

$$K_{ij} = 1.0x10^{5} \begin{pmatrix} 2.2460 & 0.3362 & 0 & 0 & 0 & 0 \\ 0.3362 & 0.9051 & 0 & 0 & 0 & 0 \\ 0 & 0 & 0.7075 & 0 & 0 & 0 \\ 0 & 0 & 0 & 0.1537 & 0.3117 & 0.0009 \\ 0 & 0 & 0 & 0.3117 & 0.1114 & 0 \\ 0 & 0 & 0 & 0.0009 & 0 & 0.2743 \end{pmatrix} \frac{lb}{in}$$

For the Kevlar-Epoxy box-beam,

$$K_{ij} = 1.0x10^{4} \begin{pmatrix} 6.1730 & 1.6152 & 0 & 0 & 0 & 0 \\ 1.6152 & 3.2138 & 0 & 0 & 0 & 0 \\ 0 & 0 & 5.8687 & 0 & 0 & 0 \\ 0 & 0 & 0 & -3.0961 & 0.1752 & 0.0010 \\ 0 & 0 & 0 & 0.1752 & 0.2920 & 0 \\ 0 & 0 & 0 & 0.0010 & 0 & 0.7316 \end{pmatrix} \frac{lb}{in}$$

4.3 Critical Temperature Difference

For the material and geometric configurations given in Figures.8-9, the critical temperature difference of the rotating cantilever box-beam is determined using the

MATLAB code generated in Appendix-A. Figure.10 shows, critical temperature difference changes with respect to the rotational speed.

Rotational Speed, RPM	Flap (ΔT), °F	Lag (ΔT), °F
0	9.88	15.38
200	10.22	15.42
500	11.86	15.61

Table 3: Critical temperature difference of the symmetric Glass-Epoxy [+45; ±45] box-beam at different rotational speeds

From the Figures 11-12, we can infer that as the rotational speed increases the critical temperature difference increases because the stiffness of the beam will increase due to the inertial forces caused by the rotation.

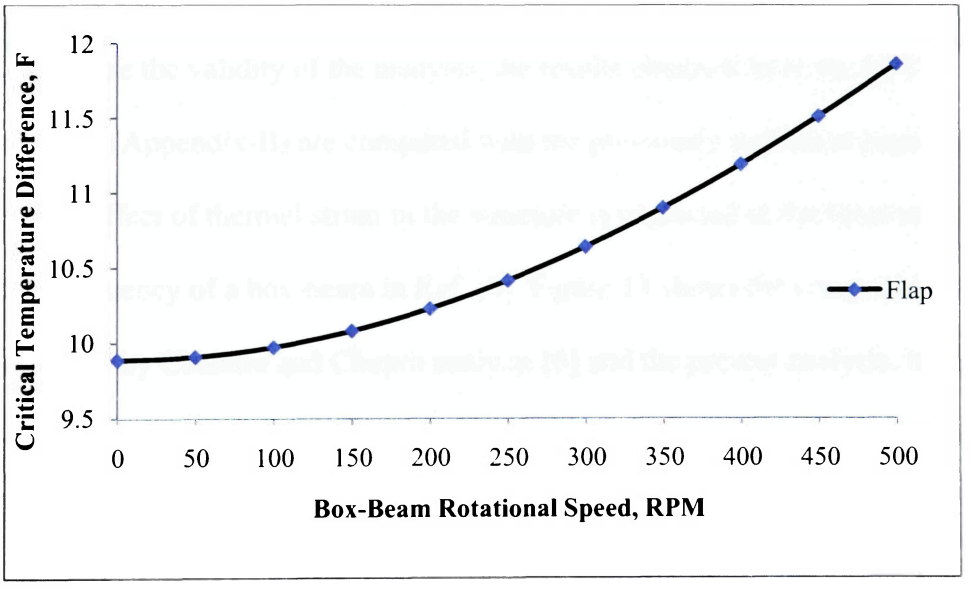

Figure 11: Critical temperature difference of a Glass-Epoxy [+45; ±45] box-beam in flap direction at different rotational speeds.

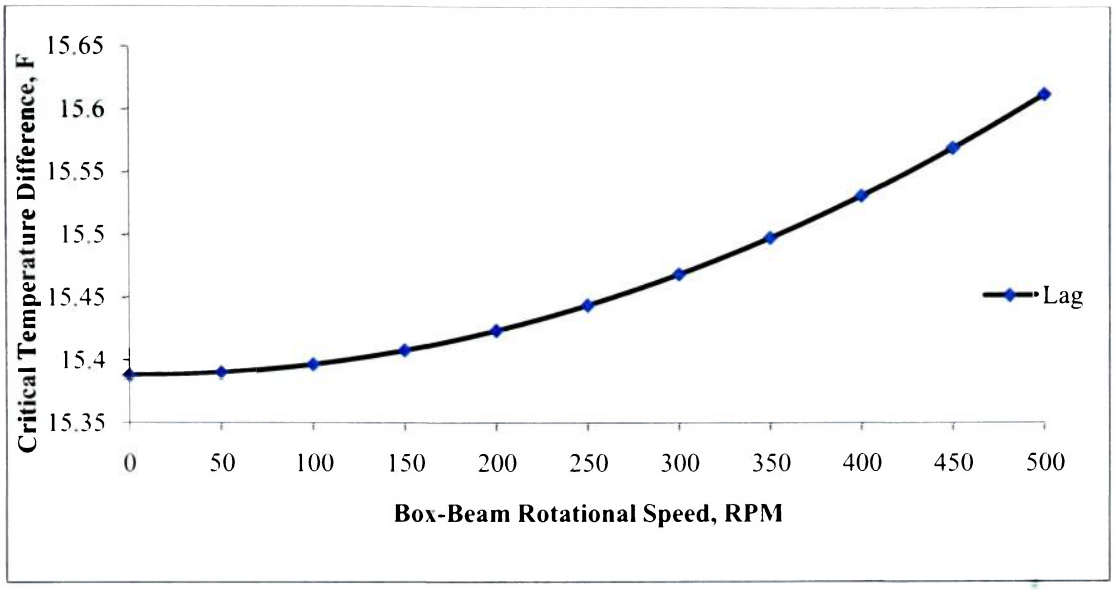

Figure 12: Critical temperature difference of a Glass-Epoxy [+45; ±45] box-beam in lag direction at different rotational speeds.

4.3 Natural Frequency

To ensure the validity of the analysis, the results obtained from the MATLAB code generated (Appendix-B) are compared with the previously published paper [6]. However, the effect of thermal strain in the structure is neglected in the determination of the natural frequency of a box-beam in Ref. [6]. Figure.13 shows the comparison of the results obtained by Chandra and Chopra analysis [6] and the present analysis. In practice, the rotational speed of a rotor blade ranges from 350 rpm to 450 rpm. The MATLAB code is executed for finding the natural frequency of the box-beam made of Glass-Epoxy and Kevlar-Epoxy with the configurations given in Tables 1- 2.

Rotational Speed, RPM	Chandra and Chopra [6], Hz	Present Analysis without Thermal Effects, Hz	Percent Difference Between Chandra and Chopra [6], and Present Analysis	Present Analysis with Thermal Effects, Hz	Percent Difference for Present Analysis with and without Thermal Effects
0	13.75	13.74	0.073%	13.02	5.38%
200	14.20	14.21	0049%	13.51	4.95%
500	16.47	16.50	0.146%	15.88	3.64%

Table 4: Comparison of natural frequency (Flap Direction) for a Glass-Epoxy [+45; ±45] box-beam for a temperature difference of 9.88°F (ΔT_{cr})

Rotational Speed, RPM	Chandra and Chopra [6], Hz	Present Analysis without Thermal Effects, Hz	Percent Difference Between Chandra and Chopra [6], and Present Analysis	Present Analysis with Thermal Effects, Hz	Percent Difference for Present Analysis with and without Thermal Effects
0	21.40	21.38	0.094%	20.92	2.16%
200	21.45	21.43	0.093%	20.97	2.15%
500	21.70	21.68	0.0692%	21.24	2.06%

Table 5: Comparison of natural frequency (Lag Direction) for a Glass-Epoxy [+45; ±45] box-beam for a temperature difference of 9.88°F (ΔT_{cr})

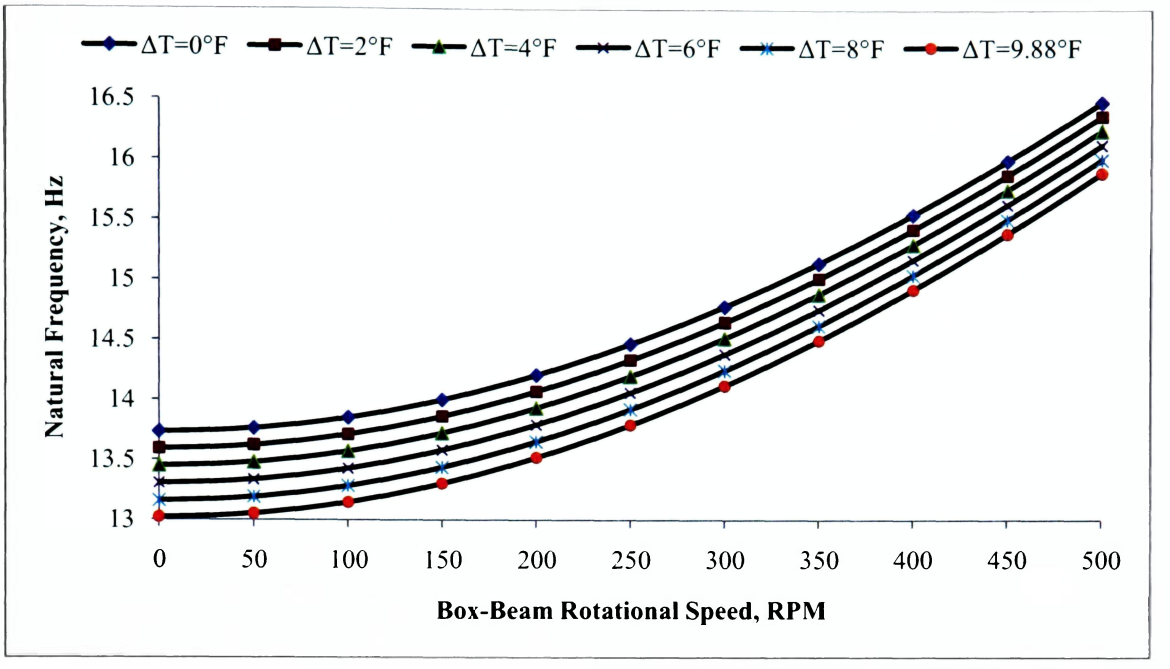

Figure 13: Natural frequency of the symmetric Glass-Epoxy [+45; ±45] box-beam with and without thermal effects in flap direction at different rotational speeds.

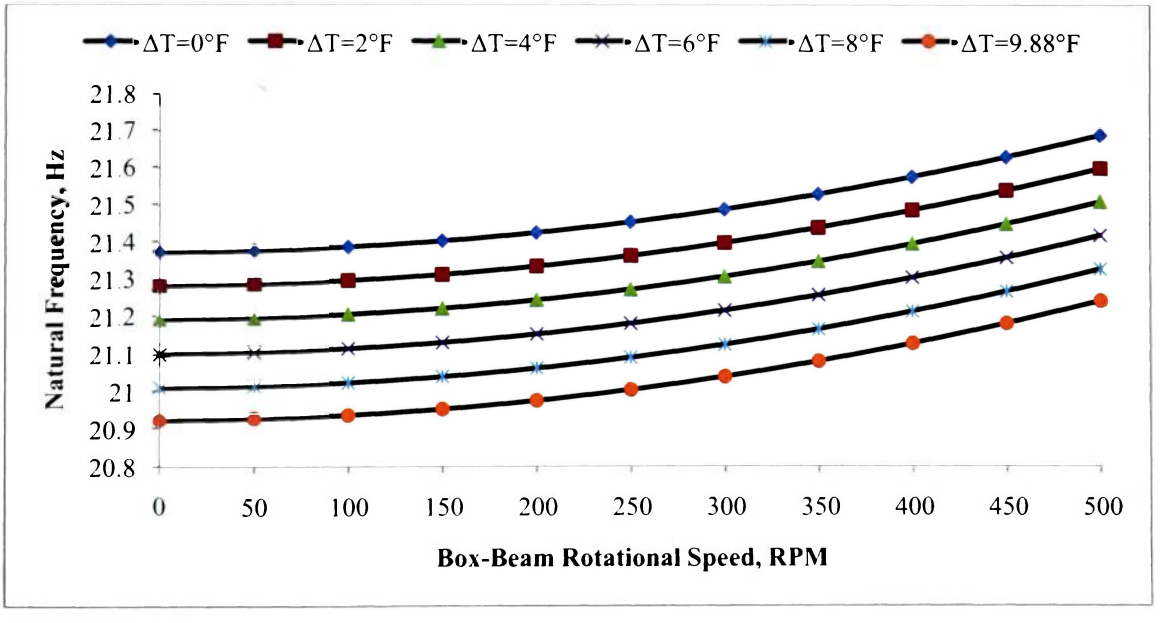

Figure 14: Natural frequency of the symmetric Glass-Epoxy [+45; ±45] box-beam with and without thermal effects in lag direction at different rotational speeds.

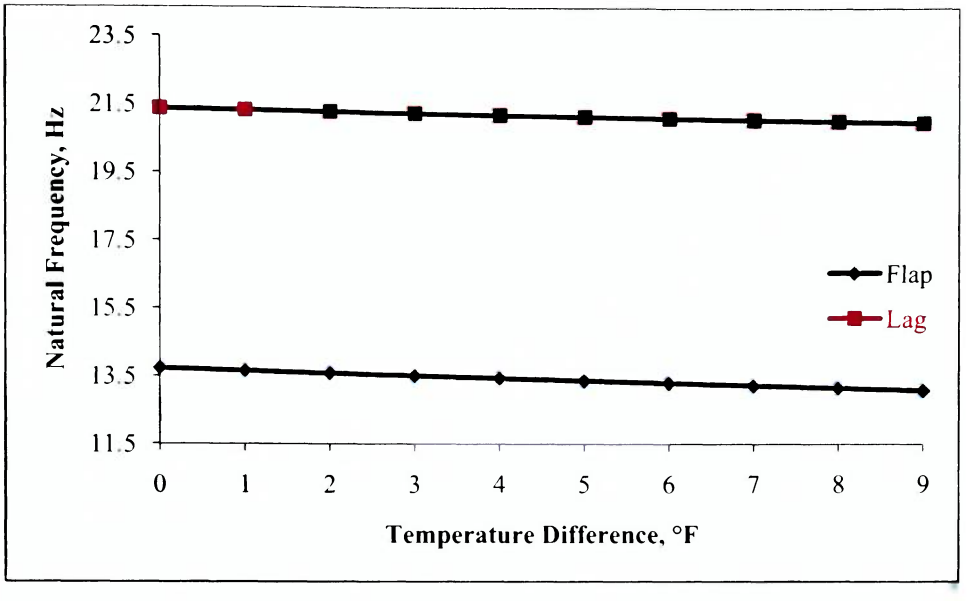

Figure 15: Variation in natural frequency of a symmetric Glass-Epoxy [+45; ±45] box-beam during the temperature change under no rotation.

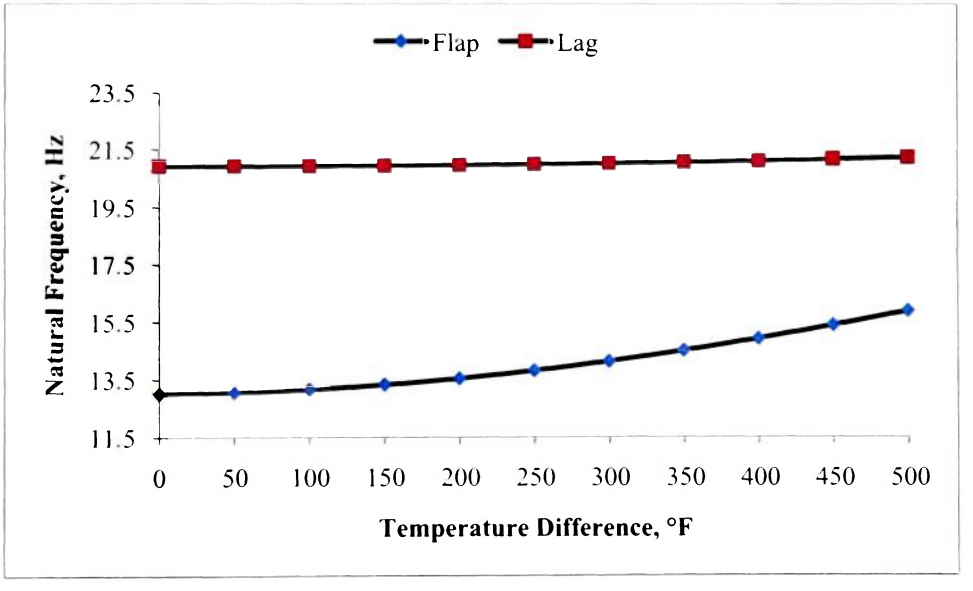

Figure 16: Natural frequency of a symmetric Glass-Epoxy [+45; ±45] box-beam for a temperature difference of 9.88°F at different rotational speeds.

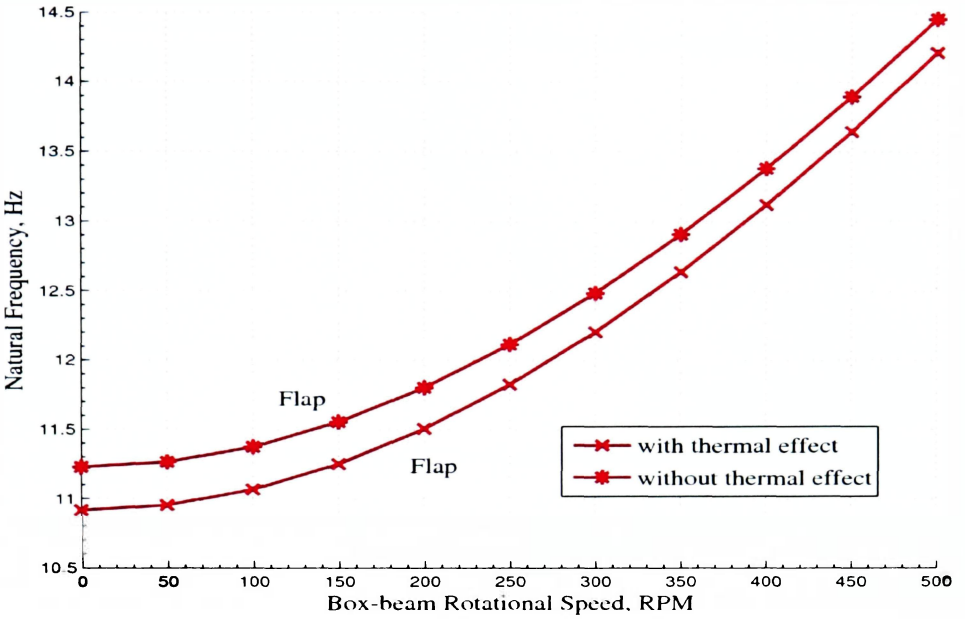

Figure 17: Natural frequency of the symmetric Kevlar-Epoxy [+45; ±45] box-beam with and without thermal effects in flap direction at different rotational speeds.

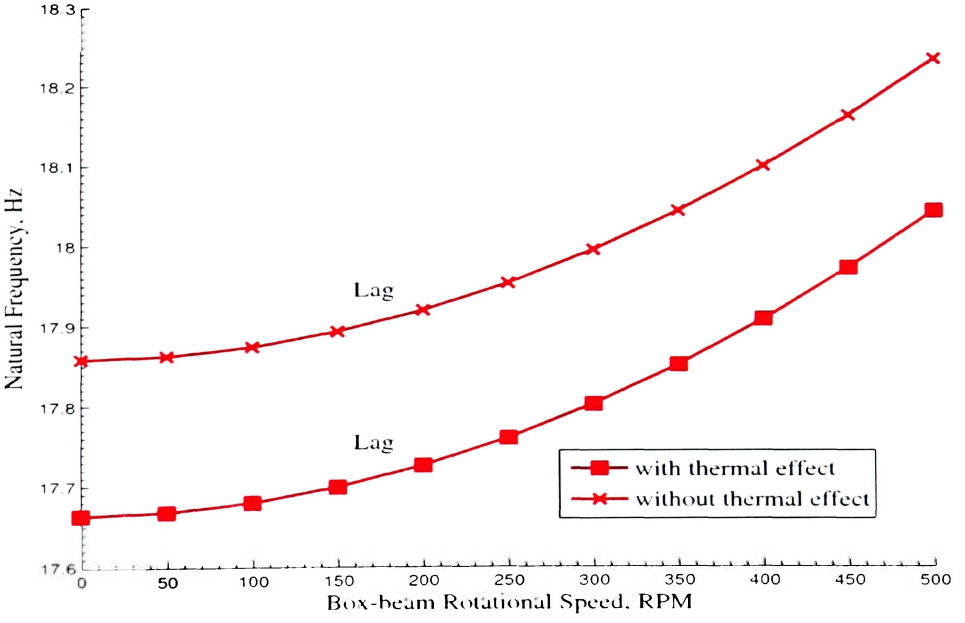

Figure 18: Natural frequency of the symmetric Kevlar-Epoxy [+45; ±45] box-beam with and without thermal effects in lag direction at different rotational speeds.

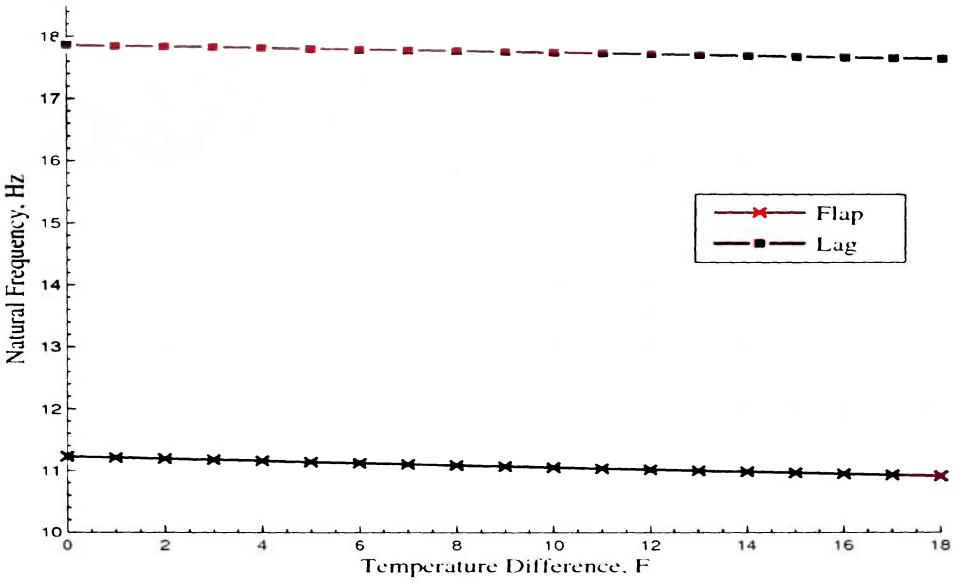

Figure 19: Variation in natural frequency of a symmetric Kevlar-Epoxy [+45; ±45] box-beam during the temperature change.

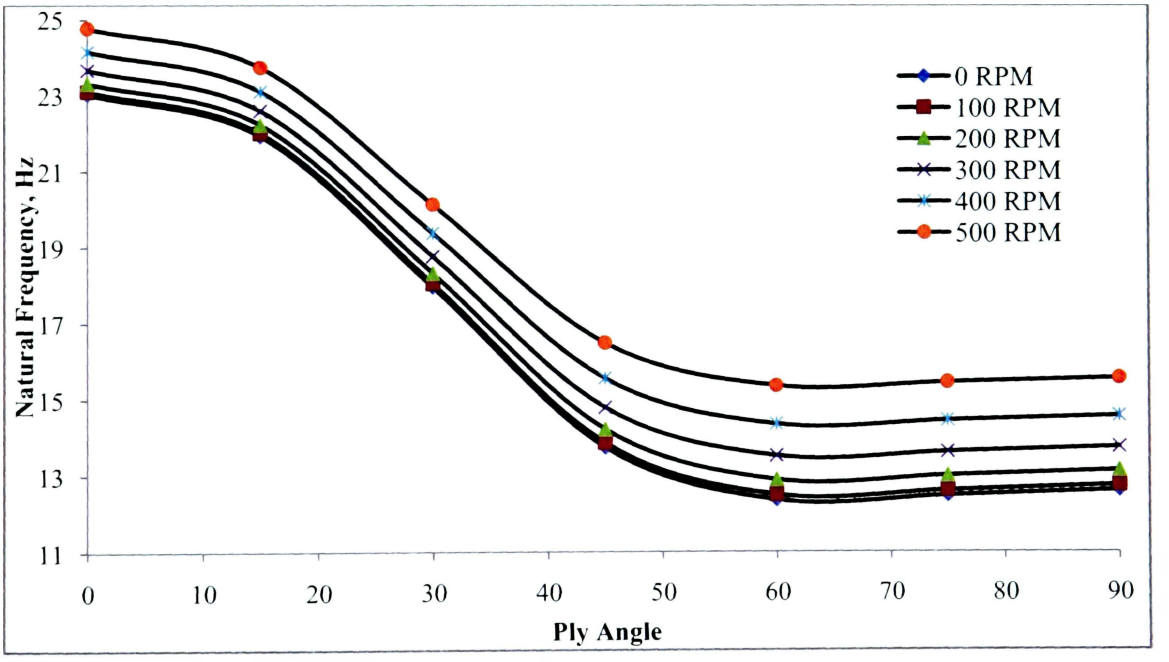

Figure 20: Variation in natural frequency (Flap Direction) of a symmetric Glass-Epoxy [+θ°; ± θ°] box-beam with the change in ply angle for different rotational speeds

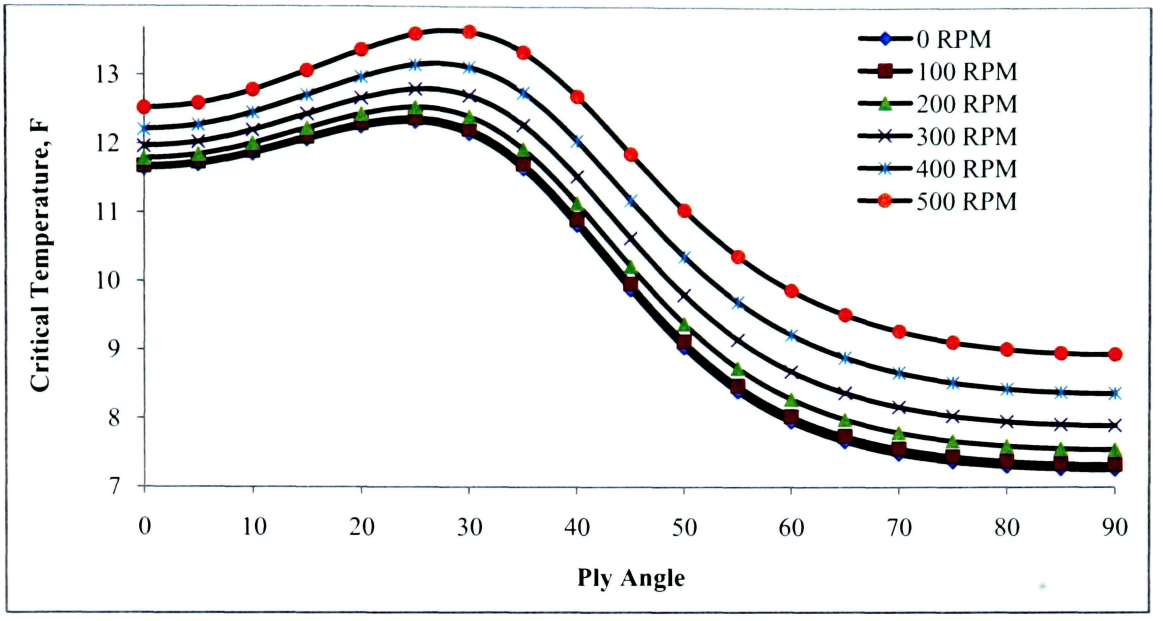

Figure 21: Variation in critical temperature (Flap Direction) of a symmetric Glass-Epoxy $[+\theta^{o}; \pm \theta^{o}]$ box-beam with the change in ply angle for different rotational speeds

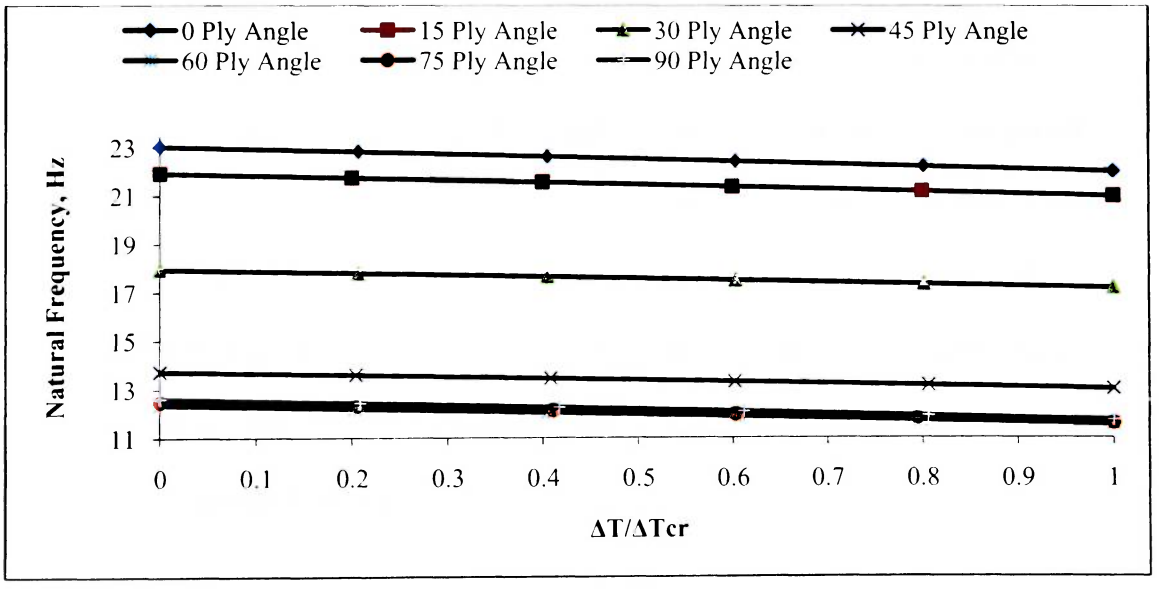

Figure 22: Variation in natural frequency (Flap Direction) of a symmetric Glass-Epoxy $[+\theta^{o}; \pm \theta^{o}]$ box-beam with the change in temperature at various ply angles

CHAPTER 5

Conclusion

Based on the above analysis, the following conclusions can be made:

1. The outcomes of the present analysis without including the thermal effects are correlated well with the Chandra and Chopra [6] results.
2. Figures 13-19 proves that the effect of thermal strain on the natural frequency of a box-beam is significant in the design of rotor blades, as the amount of decrease in the natural frequency ranges from 5.4% to 3.6% in the flap direction and the effects of thermal stress on the lag direction is not as significant. However the rotor blade assembly is a mixture of a composite box-beam and a composite honeycomb structure. So the overall effect on the natural frequency may be amplified due to the thermal stress (Table.4).
3. From Figure 22, we can infer that the change in the ply orientation angle cannot overcome the effect of thermal stress on the natural frequency of a composite box-beam.

References

1. Hodges, D. H. and Dowell, E. H., "Nonlinear Equation of Motion for the Elastic Bending and Torsion of Twisted Nonuniform Rotor Blades," NASA TN D - 7818, Dec. 1974.
2. Houbolt, J. C. and Brooks, G. W., "Differential Equations of Motion for combined Flapwise Bending, Chordwise Bending, and Torsion of Twisted Nonuniform Rotor Blades," NACA Rept. 1346, 1958.
3. Hong, C. H. and Chopra, I., "Aeroelastic Stability Analysis of a Composite Blade," *Journal of the American Helicopter Society*, Vol. 30, No. 2, 1985, pp.57–67.
4. Hong, C. H. and Chopra, I., "Aeroelastic Stability Analysis of a Composite Bearingless Rotor Blade," *Journal of the American Helicopter Society*, Vol. 31, No. 4, 1986, pp.29–35.
5. Smith. C. E. and Chopra. I., "Formulation and Evaluation of an Analytical model for Composite Box-Beams," AIAA/ASME/ASCE/AHS 31st *Structures, Structural Dynamics and Materials Conference*, Long Beach, California, April 2-4 ,1990, pp. 23-35.
6. Chandra, R. and Chopra, I., " Experimental-Theoretical Investigation of the Vibration Characteristics of Rotating Composite Box-Beams," *Journal of the American Helicopter Society*, Vol. 29, No. 4, July-August 1992, pp.657–664.
7. Anita, I. and Chopra, I., "An Analytical Model for Composite Box-Beams Including Thermal Effect," AIAA/ASME/ASCE/AHS 32nd *Structures, Structural Dynamics and Materials Conference*, Baltimore, MD, April 1991.

8. Jones, R. M., "*Mechanics of Composite Materials*," 2nd Ed. Hemisphere Publishing Corporation, 1975.
9. Rao, S. S., "Chapter 1-3," *Introduction to the Theory of Thin-Walled Structures*, Clarendon Press, Oxford, 1986.
10. Murray, N. W., "Chapter 1-3," *Introduction to the Theory of Thin-Walled Structures*, Clarendon Press, Oxford, 1986.
11. Gjelsvik, A., "Chapter 1-5," *The Theory of Thin Walled Bars*, John Wiley & Sons, New York, 1981.
12. Kollbrunner, C.F., and Basler, K., Translated from German by Glauser, E.C., "Chapter 1-3," *Torsion in Structures- An Engineering Approach*, Springer Verlag, New York, 1969.
13. Megson, T.H.G., "Chapter 5 Torsion of closed and open sections," *Linear Analysis of Thin Walled Elastic Structures*, John Wiley & Sons, New York, 1974.
14. Kaw, K. Autar, "Mechanics *of Composite Materials*," CRC Publications, Florida, 2000.

Appendix – A

Appendix – A.1 Symmetric Composite Box-Beam Stiffness Parameters

$$K_{11} = \iint_{h,v} \overline{Q}_{11} dA + a_0 \iint_{h,v} \overline{Q}_{12} dA$$

$$K_{12} = \iint_{h} \overline{Q}_{16} dA + f_0 \iint_{h} \overline{Q}_{12} dA$$

$$K_{13} = \iint_{v} \overline{Q}_{16} dA + g_0 \iint_{v} \overline{Q}_{12} dA$$

$$K_{14} = -(1+\beta) \iint_{h} \overline{Q}_{16} \zeta dA + (1-\beta) \iint_{h} \overline{Q}_{16} \eta dA + d_0 \iint_{h,v} \overline{Q}_{12} dA$$

$$K_{22} = \iint_{h} \overline{Q}_{66} dA + f_0 \iint_{h} \overline{Q}_{26} dA$$

$$K_{25} = \iint_{h} \overline{Q}_{16} \zeta dA + f_2 \iint_{v} \overline{Q}_{12} dA$$

$$K_{33} = \iint_{v} \overline{Q}_{66} dA + g_0 \iint_{v} \overline{Q}_{26} dA$$

$$K_{36} = \iint_{v} \overline{Q}_{16} \eta dA + g_1 \iint_{v} \overline{Q}_{12} dA$$

$$K_{44} = (1+\beta)^2 \iint_h \overline{Q}_{66}\zeta^2 dA + (1-\beta)^2 \iint_v \overline{Q}_{66}\eta^2 dA + d_0\left[(1-\beta)\iint_v \overline{Q}_{26}\eta dA + (1+\beta)\iint_h \overline{Q}_{26}\zeta dA\right]$$
$$+ d_1(1-\beta)\iint_v \overline{Q}_{26}\eta^2 dA - d_2(1+\beta)\iint_h \overline{Q}_{26}\zeta^2 dA$$

$$K_{45} = (1+\beta)\iint_h \overline{Q}_{16}\zeta^2 dA - d_2 \iint_{h,v} \overline{Q}_{12}\zeta^2 dA$$

$$K_{46} = -(1-\beta)\iint_v \overline{Q}_{16}\eta^2 dA - d_1 \iint_{h,v} \overline{Q}_{12}\eta^2 dA$$

$$K_{55} = \iint_{h,v} \overline{Q}_{11}\zeta^2 dA + c_2 \iint_{h,v} \overline{Q}_{12}\zeta^2 dA$$

$$K_{66} = \iint_{h,v} \overline{Q}_{11}\eta^2 dA - b_1 \iint_{h,v} \overline{Q}_{12}\eta^2 dA$$

Constants in the above stiffness parameters are

$$a_0 = -\frac{\iint_{h,v} \overline{Q}_{12} dA}{\iint_{h,v} \overline{Q}_{22} dA}$$

$$b_1 = \frac{\iint_{h,v} \overline{Q}_{12}\eta^2 dA}{\iint_{h,v} \overline{Q}_{22}\eta^2 dA}$$

$$c_2 = \frac{\iint_{h,v} \overline{Q}_{12}\zeta^2 dA}{\iint_{h,v} \overline{Q}_{22}\zeta^2 dA}$$

$$f_0 = -\frac{\iint_h \overline{Q}_{26} dA}{\iint_h \overline{Q}_{22} dA}$$

$$f_2 = -\frac{\iint_h \overline{Q}_{26} \zeta dA}{\iint_h \overline{Q}_{22} dA}$$

$$g_0 = -\frac{\iint_v \overline{Q}_{26} dA}{\iint_v \overline{Q}_{22} dA}$$

$$g_1 = -\frac{\iint_v \overline{Q}_{26} \eta dA}{\iint_v \overline{Q}_{22} dA}$$

$$d_1 = -\frac{(1-\beta)\iint_v \overline{Q}_{26} \eta^2 dA}{\iint_{h,v} \overline{Q}_{22} \eta^2 dA}$$

$$d_1 = \frac{(1+\beta)\iint_v \overline{Q}_{26} \zeta^2 dA}{\iint_{h,v} \overline{Q}_{22} \zeta^2 dA}$$

Appendix – A.2 Relation of Thermal Expansion Coefficients

Transformation of coefficient of thermal expansion from local coordinate system into global coordinate system

$$\alpha_x = \alpha_1 \cos^2(\theta) + \alpha_2 \sin^2(\theta)$$

$$\alpha_{\text{ı}} = \alpha_1 \sin^2(\theta) + \alpha_2 \cos^2(\theta)$$

$$\alpha_{xy} = -(\alpha_2 - \alpha_1) \times \cos(\theta) \times s\,\text{in}(\theta)$$